27 4-2-81 (88) 24 NTIS

SAND80-2302
TTC-0161
Unlimited Release
UC-71

(1)

R-3191

MASTER

Physical and Mechanical Properties of Cast 17-4 PH Stainless Steel

H. J. Rack
Transportation Technology Center

Prepared by Sandia Laboratories, Albuquerque, New Mexico 87185 and Livermore, California 94550 for the United States Department of Energy under Contract DE-AC04-76DP00789.

PRINTED FEBRUARY 1981

Sandia National Laboratories
energy report

SF 2900-QQB(3-80)

DISCLAIMER

Issued by Sandia Laboratories, operated for the United States Department of Energy by Sandia Corporation.

SF 1004-DF(11-77)

Printed in the United States of America
Available from
National Technical Information Service
U.S. Department of Commerce
5285 Port Royal Road
Springfield, VA 22161

NTIS price codes
Printed copy: $7.00
Microfiche copy: A01

PAGES 1 to 2

WERE INTENTIONALLY

LEFT BLANK

TTC-0161
SAND-80-2302
Unlimited Release
Printed February 1981

PHYSICAL AND MECHANICAL PROPERTIES OF CAST 17-4 PH STAINLESS STEEL*

H. J. Rack
Mechanical Metallurgy Division 5835
Sandia National Laboratories,† Albuquerque, New Mexico 87185

ABSTRACT

The physical and mechanical properties of an overaged 17-4 PH stainless steel casting have been examined. The tensile and compressive properties of cast 17-4 PH are only influenced to a slight degree by changing test temperature and strain rate. However, both the Charpy impact energy and dynamic fracture toughness exhibit a tough-to-brittle transition with decreasing temperature--this transition being related to a change in fracture mode from ductile, dimple to cleavage-like. Finally, although the overaged 17-4 PH casting had a relatively low room temperature Charpy impact energy when compared to wrought 17-4 PH, its fracture toughness was at least comparable to that of wrought 17-4 PH. This observation suggests that prior correlations between Charpy impact energies and fracture toughness, as derived from wrought materials, must be approached with caution when applied to cast alloys.

*This work sponsored by the U. S. Department of Energy under Contract DE-AC04-76-DP00789.

†A U. S. Department of Energy facility.

ACKNOWLEDGMENT

The author wishes to acknowledge the assistance of J. C. Rowe, R. Blose and M. Sturm in the mechanical testing and scanning electron microscopy portions of this program.

CONTENTS

This Page Intentionally Left Blank.

INTRODUCTION

Prior studies of 17-4 PH stainless steel (1-11) have generally considered the mechanical and physical properties of wrought product forms, that is rolled plate, forgings, etc. There are, however, many instances where, because of economic considerations, 17-4 PH stainless steel castings might be an attractive alternative. Unfortunately, little information exists on the mechanical and physical properties of 17-4 PH stainless steel castings. This report presents the results of an evaluation of such a casting. Where available, direct comparison with data obtained from wrought 17-4 PH stainless steel is also included.

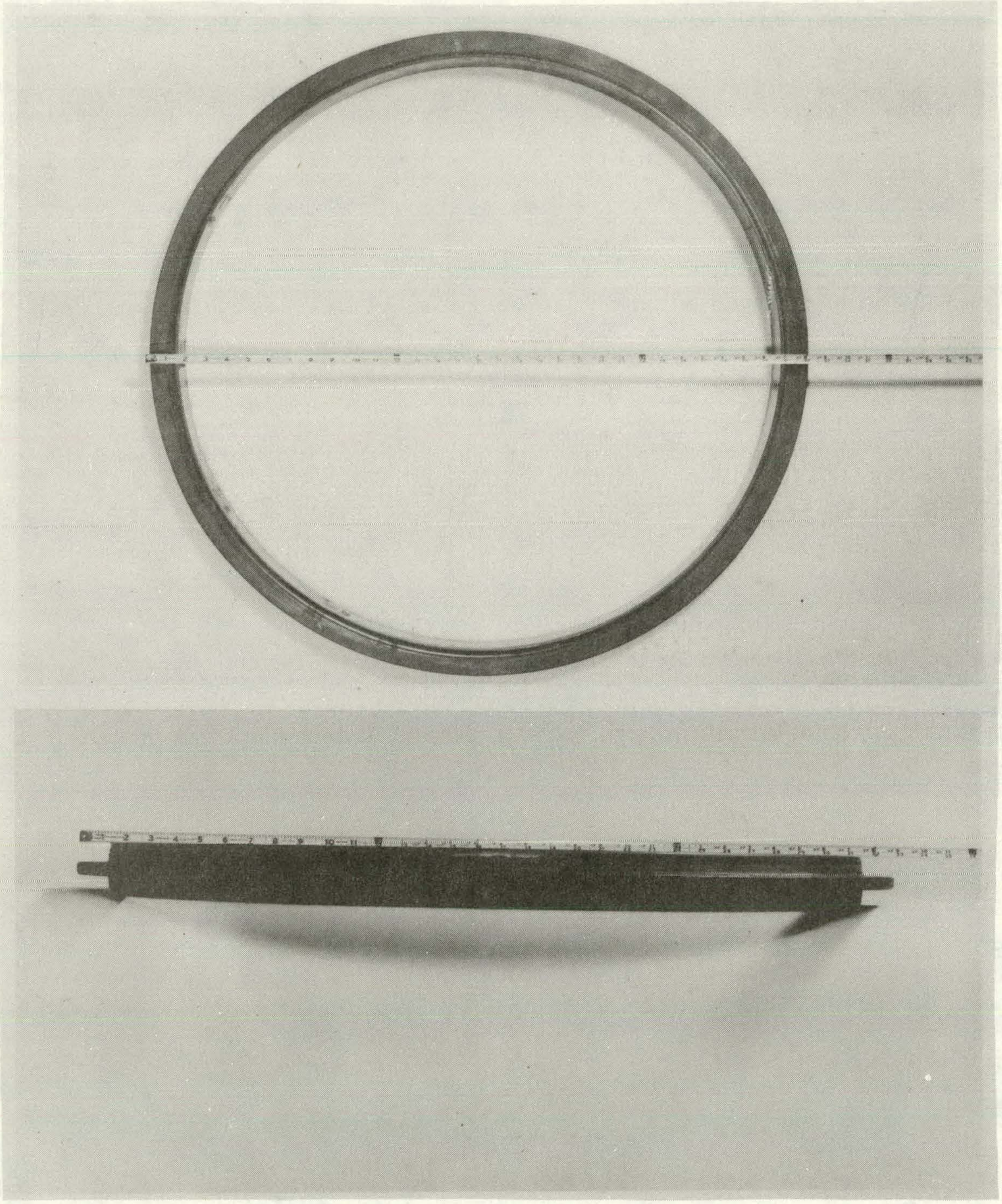

Figure 1. Top and Side Views of 17-4 PH Stainless Steel Seal Casting.

EXPERIMENTAL PROCEDURE

Figure 1 shows the 17-4 PH stainless steel casting evaluated in this study. This casting was selected since it is currently being considered as the primary metallic seal for a liquid metal breeder reactor spent fuel shipping container. As such, the seal must operate at temperatures between 233 and 473K. In addition, it must be able to withstand applied strain rates approaching 10 sec^{-1}.

Physical Properties

Physical property measurements of the 17-4 PH stainless steel casting involved determinations of the linear expansion, specific heat and thermal diffusivity as a function of temperature. A dual fused silica pushrod Theta dilatometer* operating in a room temperature environment was used to obtain linear expansion measurements in the temperature range 298 to 1173K (12). Measurements between 298 to 217K were made with a single fused silica pushrod dilatometer, again maintained in a room temperature environment. Finally, the linear expansion samples, 25.4 mm in length x 2.54 mm square, were equilibrated for one hour at each test temperature prior to expansion measurements.

Specific heat determinations utilized a Perkin Elmer Model DSC 2 differential scanning calorimeter connected to a PRL minicomputer-based digital data acquisition system (13). The thermal diffusivity results were obtained using a computer controlled laser flash diffusivity technique (13). Knowing the specific heat, C_p and the thermal diffusivity α, the thermal conductivity, λ, was then calculated from

$$\lambda = \alpha \rho C_p \tag{1}$$

where ρ is the density corrected for changes in temperature relative to room temperature (298K).

*The dilatometer was calibrated using standard fused silica and platinum samples.

Mechanical Behavior

The elastic properties of the 17-4 PH stainless steel casting were measured over the temperature range 233 to 1073K using standard ultrasonic techniques (14). These techniques require that the travel time, t, for an ultrasonic wave to propagate through a known specimen length, L, be obtained as a function of temperature. Once this travel time is known, the ultrasonic velocity, V, can be determined from

$$V = L/t$$

where the length L is corrected for temperature changes using the thermal expansion data described above. The elastic moduli were calculated from the longitudinal velocity, V_L, and the shear velocity, V_s, from

$$G = \rho V_s^2 \tag{2}$$

$$E = 2G(1 + \nu) \tag{3}$$

$$\nu = \frac{\left[1 - \frac{1}{2} V_L^2/V_s^2\right]}{\left[1 - V_L^2/V_s^2\right]} \tag{4}$$

where G, E, ν and ρ are the shear moduli, Young's moduli, Poisson's ratio and density, respectively. Again, the latter was corrected for changes due to increasing/decreasing temperature about 298K.

The plastic behavior of the 17-4 PH stainless steel casting was evaluated using standard tensile, compression and Charpy (blunt V-notch and fatigue precracked) test procedures. Figure 2 illustrates the location of these samples as removed from the 17-4 PH stainless steel seal casting.* Tensile and compression tests were performed between strain rates of 1.3×10^{-6} and $1.2\ \text{sec}^{-1}$ over a temperature range 215 to 435K.

*The actual sample configurations are given in more detail in Appendix A.

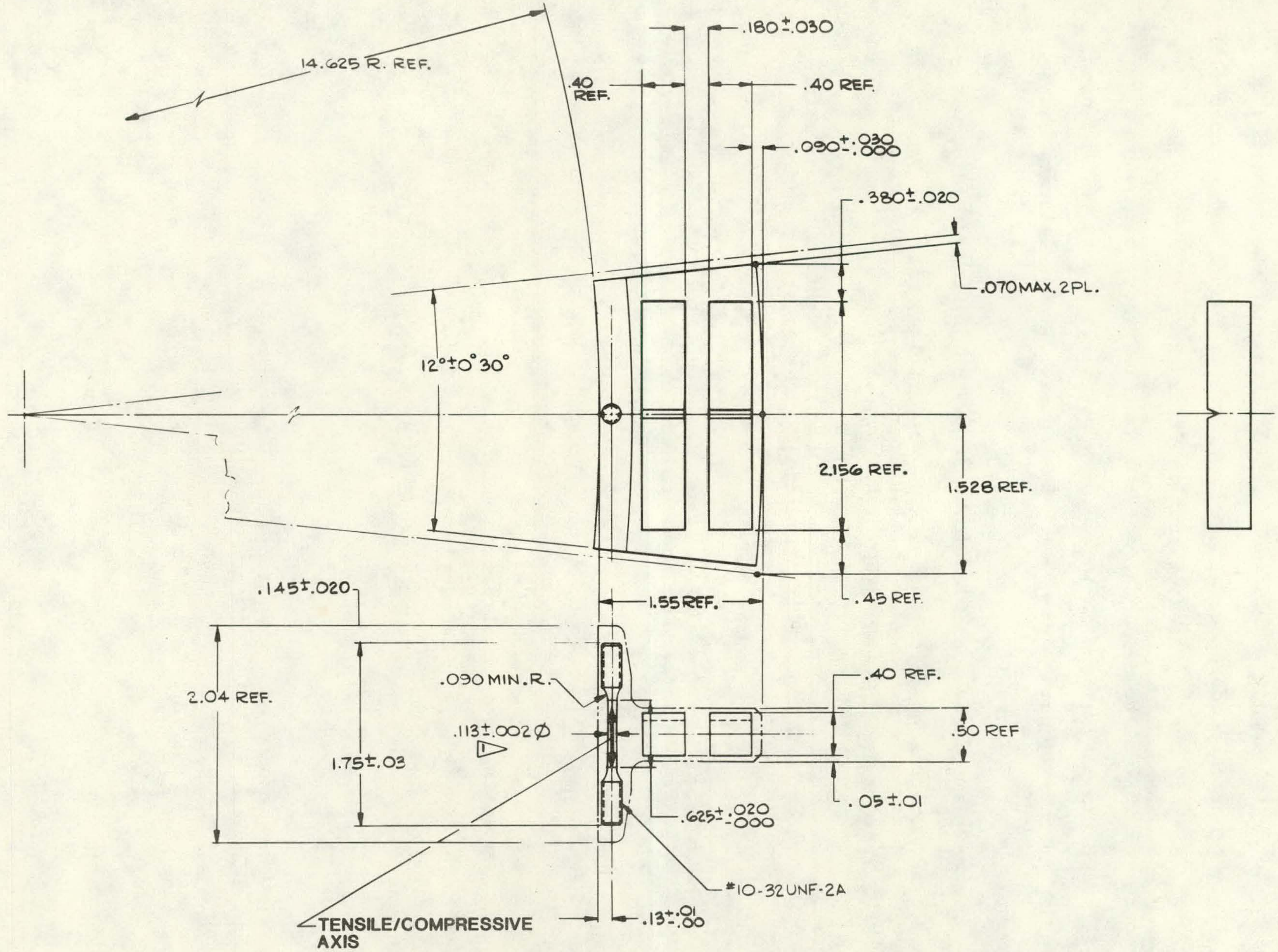

Figure 2. Mechanical Property Specimen Location in 17-4 PH Stainless Steel Seal Casting (1 in = 25.4 cm).

The Charpy impact samples were tested in either the V-notched or fatigue precracked condition. Fatigue precracking utilized methods (15) where the final stress intensity during precracking, K_f, was always controlled at less than one-half of the dynamic fracture toughness, K_d. Both the notched and fatigue precracked samples were tested using an instrumented impact machine with the initial impact velocity being maintained at 3.3 m/s (16,17).

When the fracture was elastic, that is, no general yielding was observed, the fracture toughness, K_{Id}, was obtained from the precracked Charpy samples as calculated from (18):

$$K_{Id} = \frac{4P_M}{BW^{1/2}} \left[2.9\left(\frac{a}{W}\right)^{1/2} - 4.6\left(\frac{a}{W}\right)^{3/2} + 21.8\left(\frac{a}{W}\right)^{5/2} - 37.6\left(\frac{a}{W}\right)^{7/2} + 38.7\left(\frac{a}{W}\right)^{9/2} \right] \tag{5}$$

where P_M is the maximum load, B = W = 10 mm, and a is the crack length. When general yielding was observed, i.e., at the higher test temperatures, an estimate of the fracture toughness was obtained from a knowledge of the energy-based value of the J integral, i.e.,

$$K_{JD} = (EJ_{Id})^{1/2} \tag{6}$$

where J_{ID} is given by

$$J_{ID} = 2E_M/Bb \tag{7}$$

where b = W - a and E_M was taken as the true specimen energy to maximum load (18).

RESULTS AND DISCUSSION

General

The chemical composition of the 17-4 PH stainless steel casting examined in this study is given in Table 1. Before machining, this casting had been homogenized at 1422K and then solution treated at 1311K. Final aging involved a four hour exposure at 922K. Optical microscopy indicated that the casting possessed an aged α-martensite matrix with δ-ferrite stringers, Figure 3. High magnification examination of the α-martensite matrix, Figure 4, indicated that the casting was in the overaged heat treatment condition; that it contained a rather coarse dispersion of the primary strengthening phase, spherical face centered cubic Cu particles. Further examination, Figure 5, revealed the presence of rod-shaped precipitates within the δ-ferrite stringers. X-ray energy dispersive analysis, Figure 6, indicated that these particles were relatively rich in Cu when compared to the δ-ferrite matrix. The appearance of these rod-shaped Cu rich particles within the δ-ferrite stringers seems to be restricted to 17-4 PH stainless steel castings since their presence has not been reported in previous studies of wrought 17-4 PH stainless steel (1-11).

Table 1

Chemical Composition of 17-4 PH Casting

Element	Weight Percent
Cr	16.94
Ni	4.0
Cu	3.0
Mn	0.5
C	0.044
S	0.022
Si	0.7
Nb	0.3
Fe	Bal.

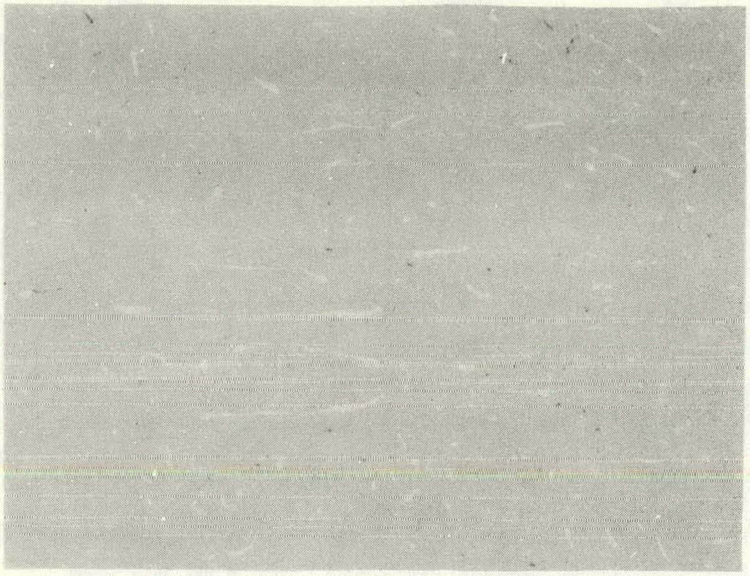

Figure 3. Optical Micrograph of 17-4 PH Stainless Steel Casting. White Areas δ-Ferrite Stringers; Darker Matrix Aged α-Martensite. Original Magnification 100X.

Figure 4. Transmission Electron Micrograph of Aged α-Martensite in 17-4 PH Stainless Steel Casting Containing Spherical Cu Precipitates. Original Magnification: 40,000X.

Figure 5. Transmission Electron Micrograph of δ-Ferrite Stringer Containing Rod-Shaped Cu-Rich Precipitate. Original Magnification: 52,000X.

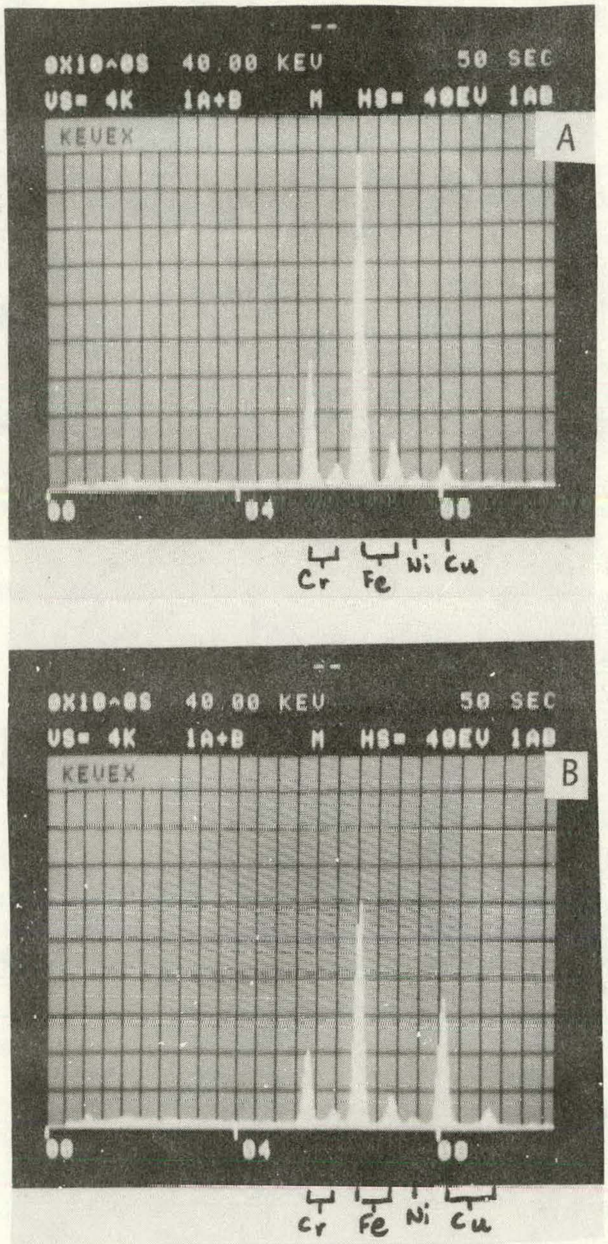

Figure 6. X-Ray Energy Dispersive Spectra From (a) δ-Ferrite Matrix and (b) Rod-Shaped Particles Shown in Fig. 5.

Physical Properties

The results of the thermal expansion measurements are tabulated in Table 2 and plotted in Figure 7. This figure shows that the thermal linear expansion of the 17-4 PH stainless steel casting, as represented by the individual data points, agreed quite well with the average linear expansion data previously obtained for wrought 17-4 PH stainless data (19-21), the latter being described by the dashed line in Figure 7.

This agreement between the properties of wrought and cast 17-4 PH stainless steel was not observed when the thermal properties were considered. The results of the specific heat and thermal diffusivity measurements are tabulated in Tables 3 and 4, respectively, with the corresponding calculated values of the thermal conductivity being presented in Table 5. This tabulated data is plotted in Figures 8 through 10, with the dashed lines in Figures 8 and 10 representing the average of previous data obtained from wrought 17-4 PH stainless steel (21). In general, these results indicate that the thermal properties of cast 17-4 PH stainless steel appear to be much more sensitive to changes in temperature than would be expected from the wrought 17-4 PH stainless steel data. Comparison of typical microstructures from cast and wrought 17-4 PH stainless steel suggests that this difference between the two products may be due to the increased volume fraction of δ-ferrite in cast 17-4 PH relative to that in the wrought alloy.

Table 2

Thermal Linear Expansion of 17-4 PH
Stainless Steel Casting

Temperature (K)	$\Delta L/L_o$ (Pct)
279	-0.030
298	0.000
474	0.194
476	0.199
568	0.313
626	0.373
627	0.372
643	0.409
776	0.546
781	0.562
783	0.566
917	0.711
919	0.671
925	0.703
1064	0.824
1212	1.107

Table 3

Specific Heat of 17-4 PH Stainless Steel Casting

Temperature (K)	Specific Heat (W sec gm^{-1} K^{-1})
350	0.4750
375	0.4884
400	0.4973
425	0.5054
450	0.5147
460	0.5220
475	0.5228
500	0.5335
525	0.5396
550	0.5477
575	0.5548
600	0.5636
625	0.5726
650	0.5805
675	0.5885
700	0.5978
725	0.6080
750	0.6343
775	0.6594
795	0.6812
800	0.6875
825	0.7246
850	0.7409
875	0.7576
900	0.7672
925	0.7789

Table 4

Thermal Diffusivity of 17-4 PH Stainless Steel Casting

Temperature (K)	Diffusivity (cm^2 sec^{-1})
294	0.0458
461	0.0452
627	0.0457
794	0.0430
961	0.0475
1127	0.0548

Table 5

Thermal Conductivity of 17-4 PH Stainless Steel Casting

Temperature (K)	Conductivity (W cm^{-1} K^{-1})
294	0.152
461	0.180
627	0.199
794	0.206
961	0.281

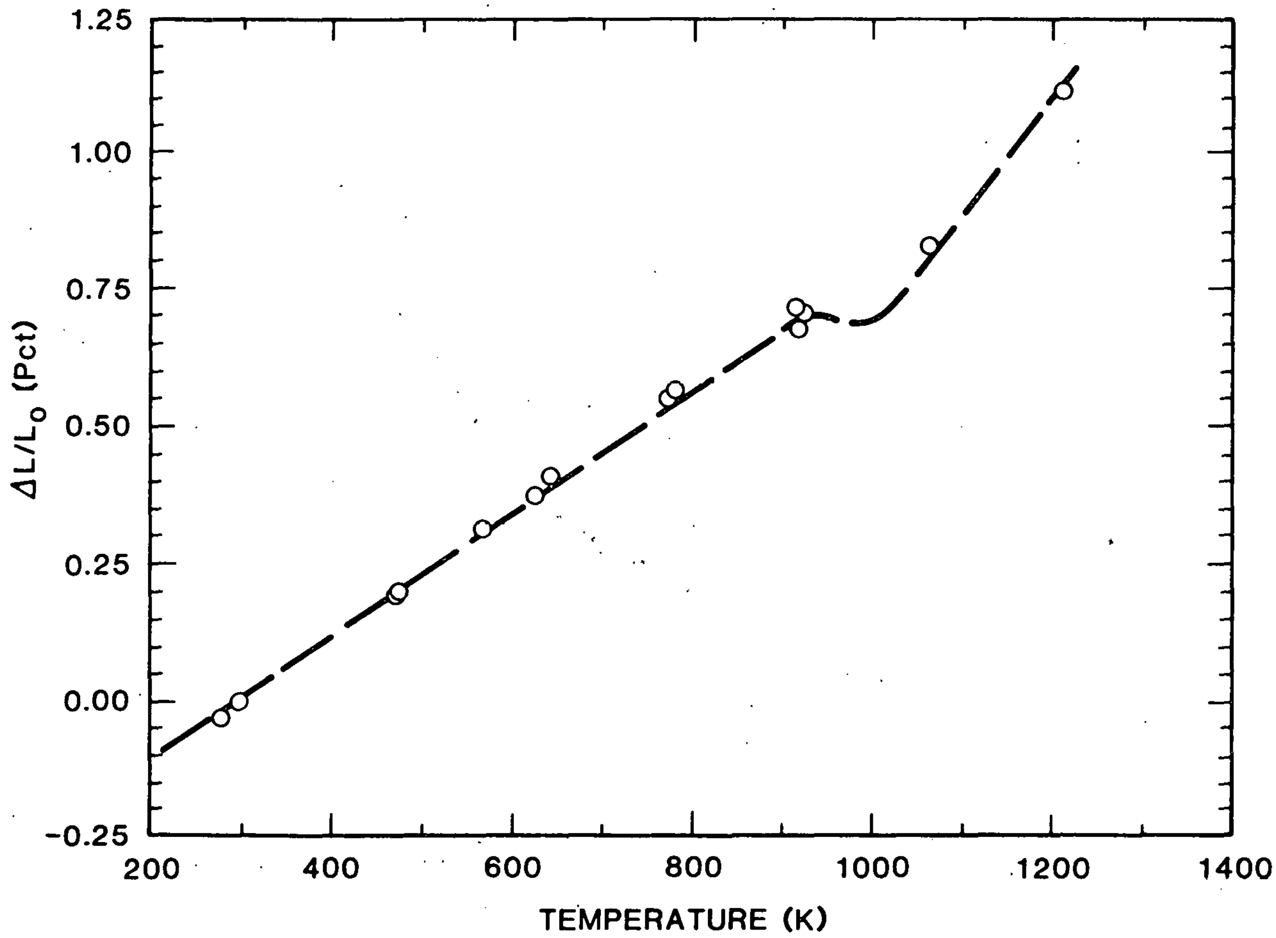

Figure 7. Linear Thermal Expansion of 17-4 PH Stainless Steel. Data Points from 17-4 PH Casting, Dashed Line an Average Obtained from Wrought 17-4 PH Stainless Steel (19-21).

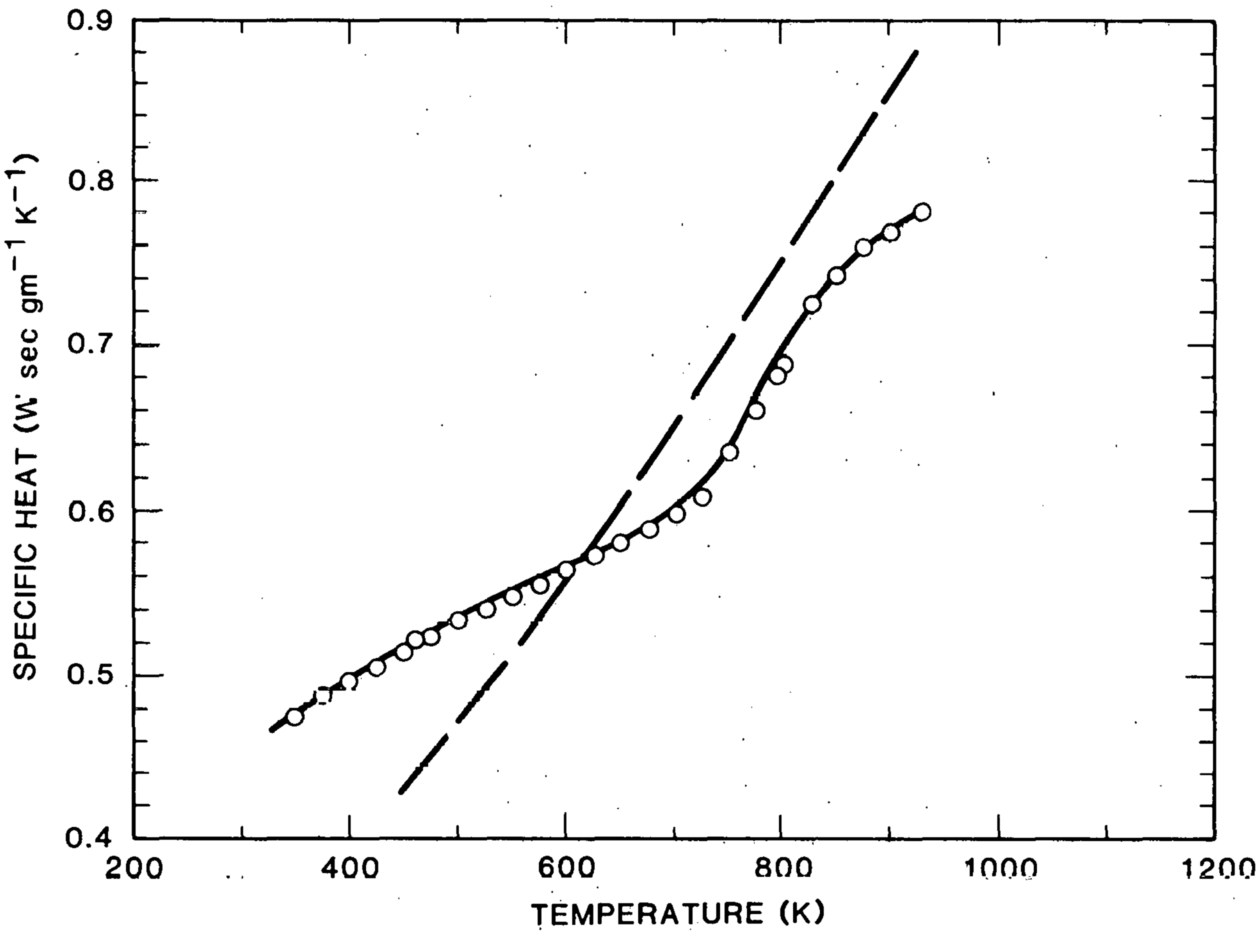

Figure 8. Specific Heat of 17-4 PH Stainless Steel as a Function of Temperature. Data Points from 17-4 PH Casting, Dashed Line an Average Obtained from Wrought 17-4 PH Stainless Steel (21).

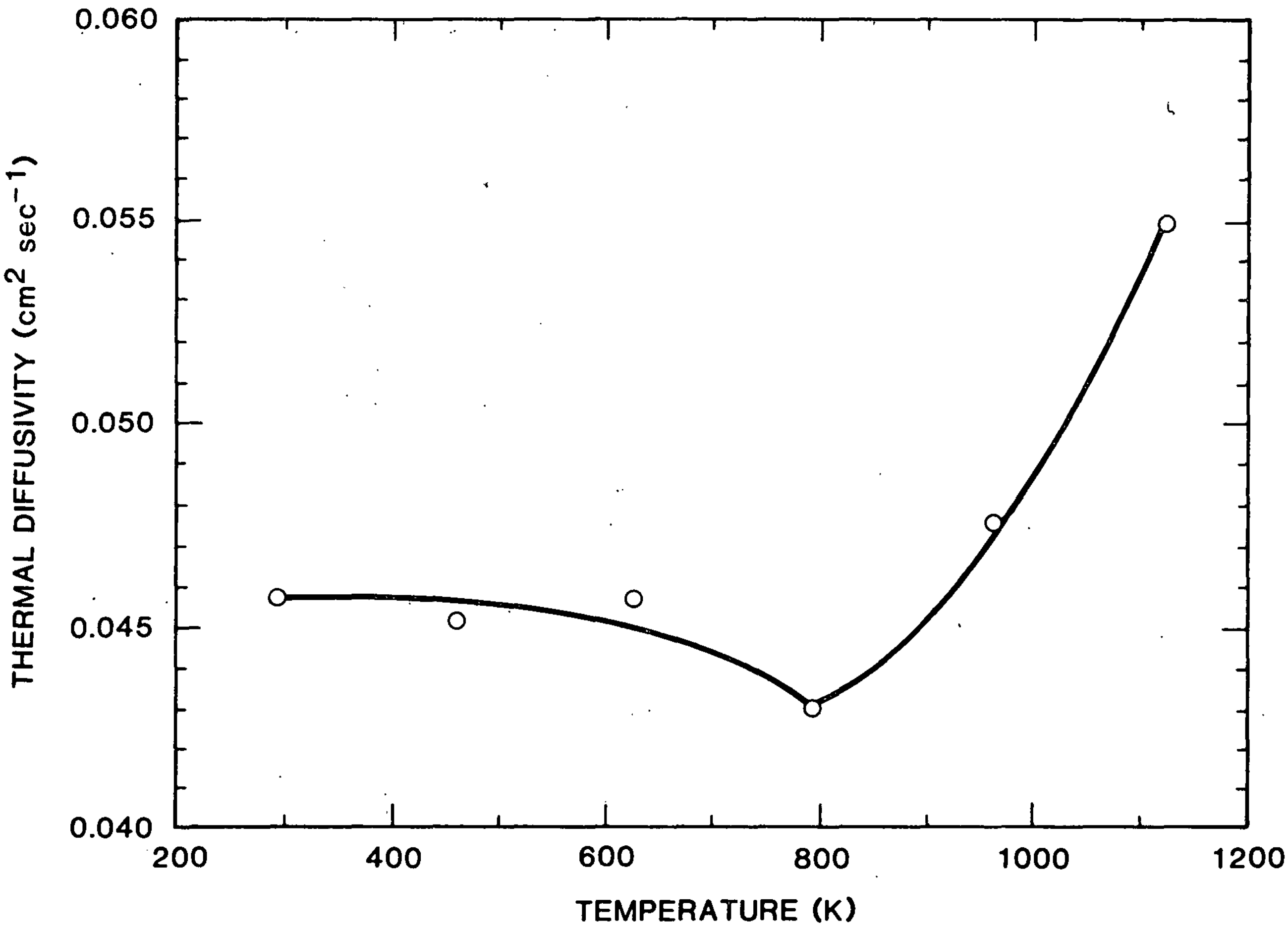

Figure 9. Thermal Diffusivity of Cast 17-4 PH Stainless Steel as a Function of Temperature.

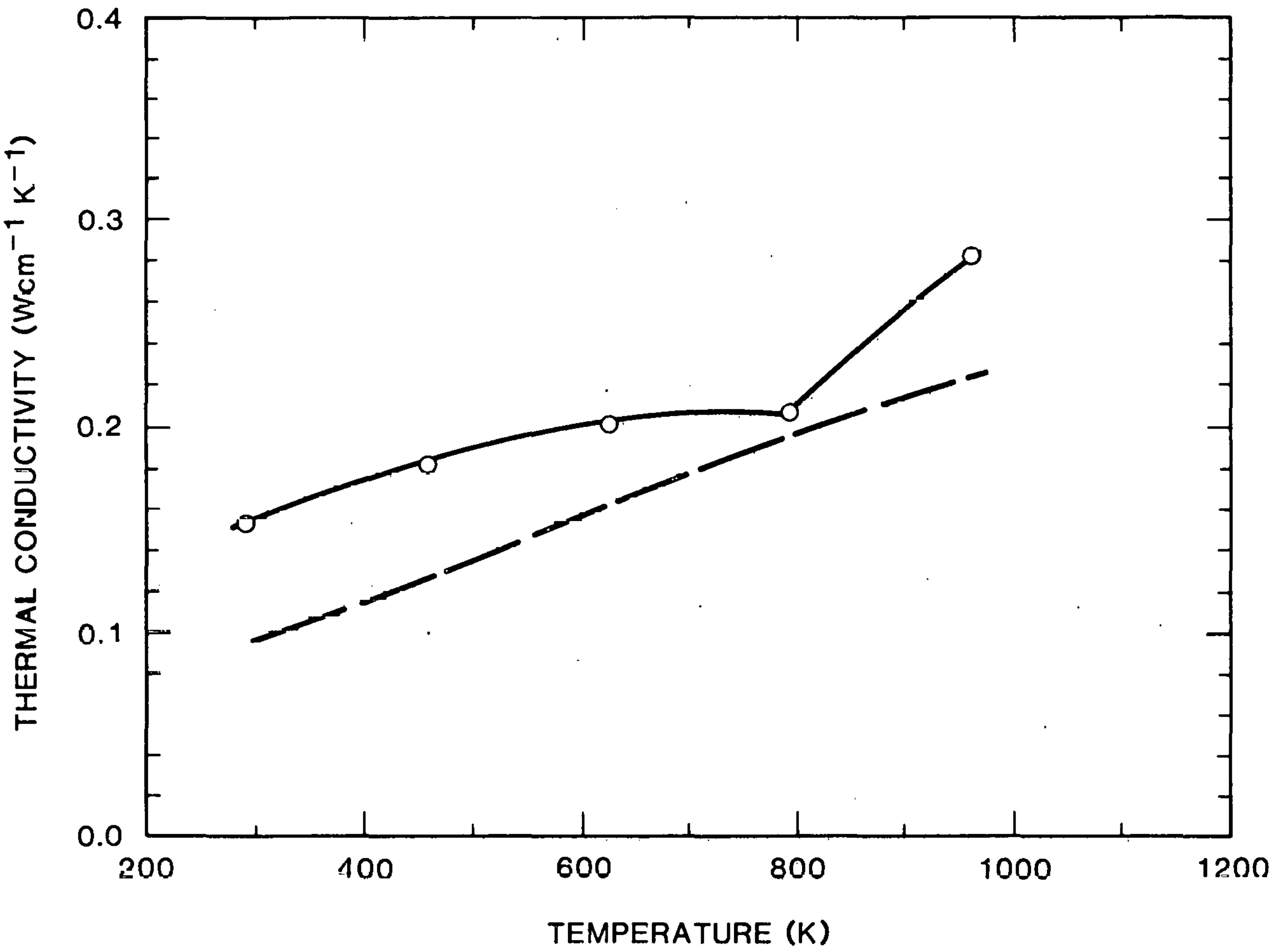

Figure 10. Thermal Conductivity of 17-4 PH Stainless Steel as a Function of Temperature. Data Points from 17-4 PH Casting, Dashed Line an Average Obtained from Wrought 17-4 PH Stainless Steel (21).

Mechanical Behavior

The elastic properties of the overaged 17-4 PH stainless steel casting as a function of temperature are tabulated in Tables 6 and 7 and plotted in Figure 11. Typical values of the Young's modulus, shear modulus and Poisson's ratio for wrought 17-4 PH stainless steel have also been included in this figure. In general, the agreement between the room temperature values of the Young's modulus and Poisson's ratio for cast and wrought 17-4 PH stainless steel was quite good. However, the measurements of the shear modulus and the elevated temperature Young's moduli for the 17-4 PH casting all tended to be higher than those reported for wrought 17-4 PH stainless steel. Notwithstanding these differences the results all indicate that both the Young's moduli and the shear moduli decrease with increasing temperature.

Representative tensile and compressive stress-strain curves for the overaged 17-4 PH stainless steel casting are presented in Appendices B and C. The influences of test temperature and strain rate on selected plastic properties of the 17-4 PH stainless steel casting have been summarized in Figures 12 and 13. These results show that above a critical temperature, T_c, the compressive and tensile yield strengths are essentially independent of both test temperature and strain rate. Below T_c, the compressive and tensile yield strengths increase with either decreasing temperature or increasing strain rate. Finally, the rate of compressive and tensile yield strength increase with test temperature below T_c is a function of strain rate. For example, at slow strain rates, e.g., $1.6 \times 10^{-4} s^{-1}$ in tension, the rate of increase $d\sigma/dT$ was -0.44 MPa/K, while at high strain rates, e.g., $1.2\ s^{-1}$ in tension, the rate of increase was -0.88 MPa/K.

The tensile ductility, as represented by the uniform elongation and the total elongation, was, to some degree, a function of test

Table 6

Young's Modulus and Poisson's Ratio
of 17-4 PH Casting

Temperature (K)	Young's Modulus (GPa)	Poisson's Ratio
248	211.0	0.283
297	204.2	0.291
298	204.1	0.291
301	202.8	0.288
494	194.6	0.295
501	191.5	0.296
580	186.7	0.296
582	186.2	0.294
650	182.2	0.306
650	181.9	0.304
728	176.3	0.316
742	174.0	0.307
798	167.8	0.309
817	164.7	0.321
885	153.3	0.322
957	142.3	0.332
1031	134.0	0.344
1067	128.8	0.348
1151	118.0	0.359
1162	117.3	0.361

Table 7

Shear Modulus of 17-4 PH Casting

Temperature (K)	Shear Modulus (GPa)
249	82.18
298	79.07
301	78.73
382	76.32
495	74.94
523	70.53
568	69.97
582	71.9
632	68.73
675	68.8
696	67.01
749	65.42
777	64.1
793	64.39
841	59.91
881	57.63
885	59.98
934	54.39
982	52.26
1028	49.78
1077	47.50

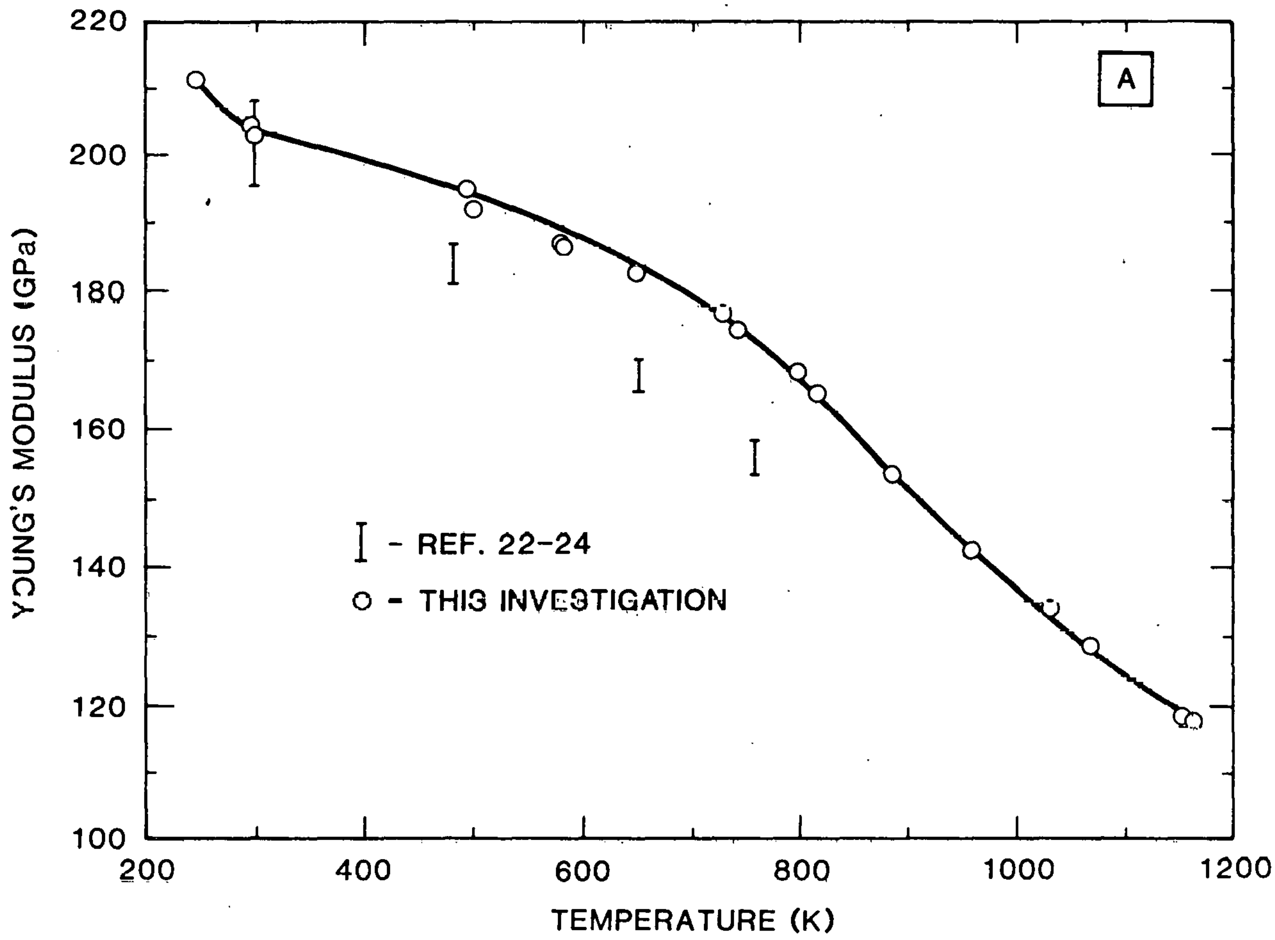

Figure 11. Elastic Properties of Overaged 17-4 PH Stainless Steel Casting (a) Young's Modulus, (b) Shear Modulus and (c) Poisson's Ratio.

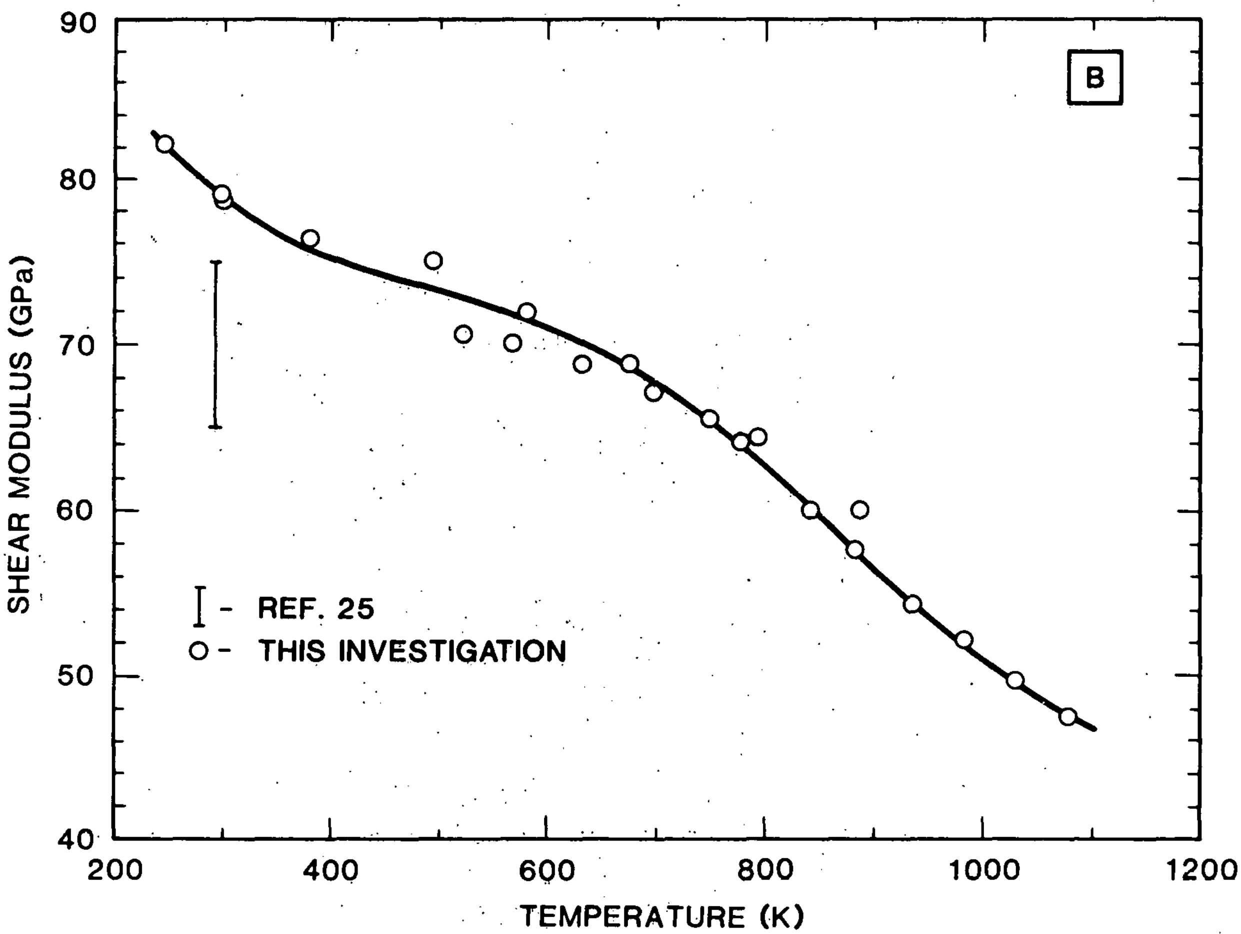

Figure 11. (Cont'd)

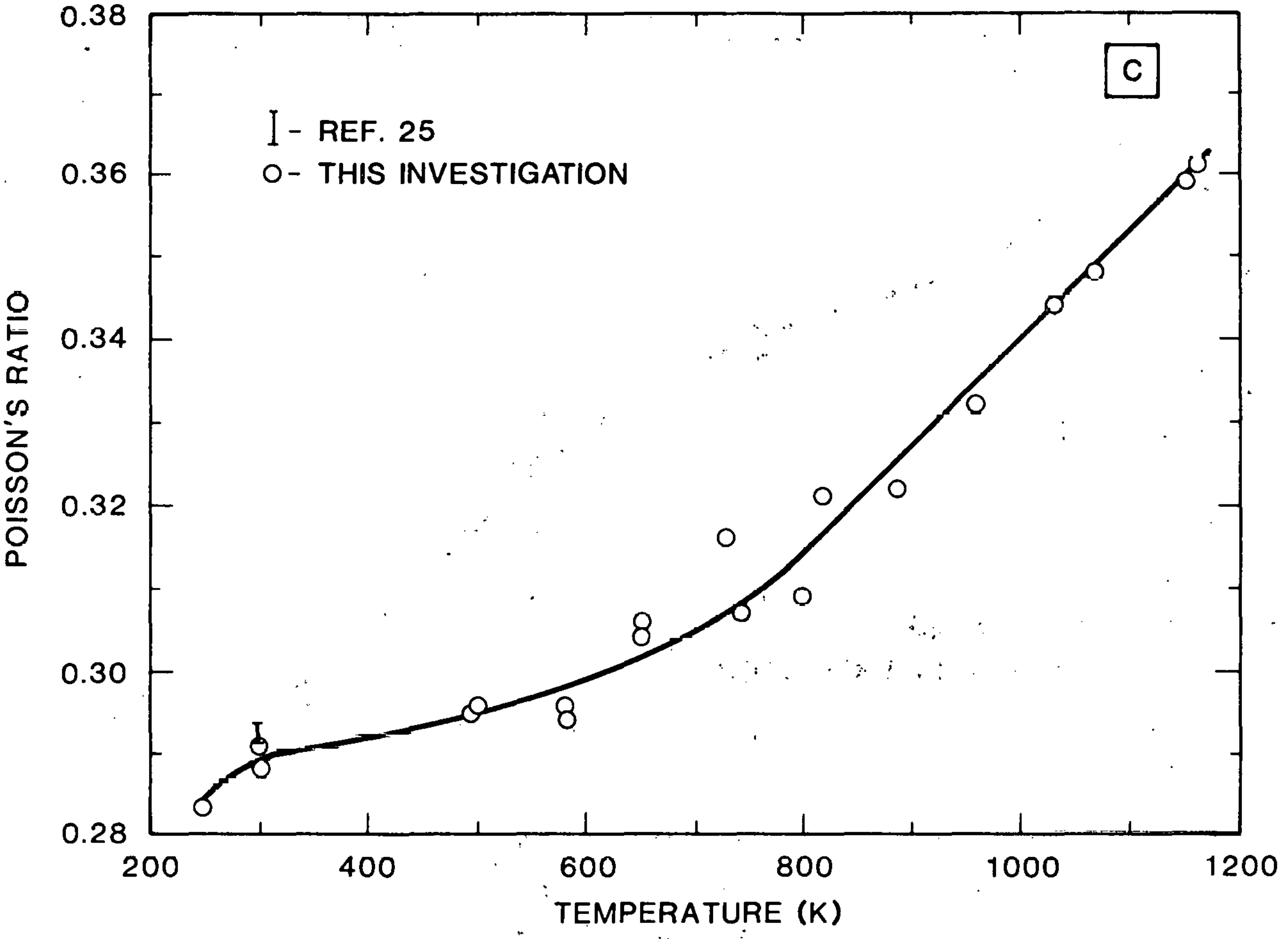

Figure 11. (Cont'd)

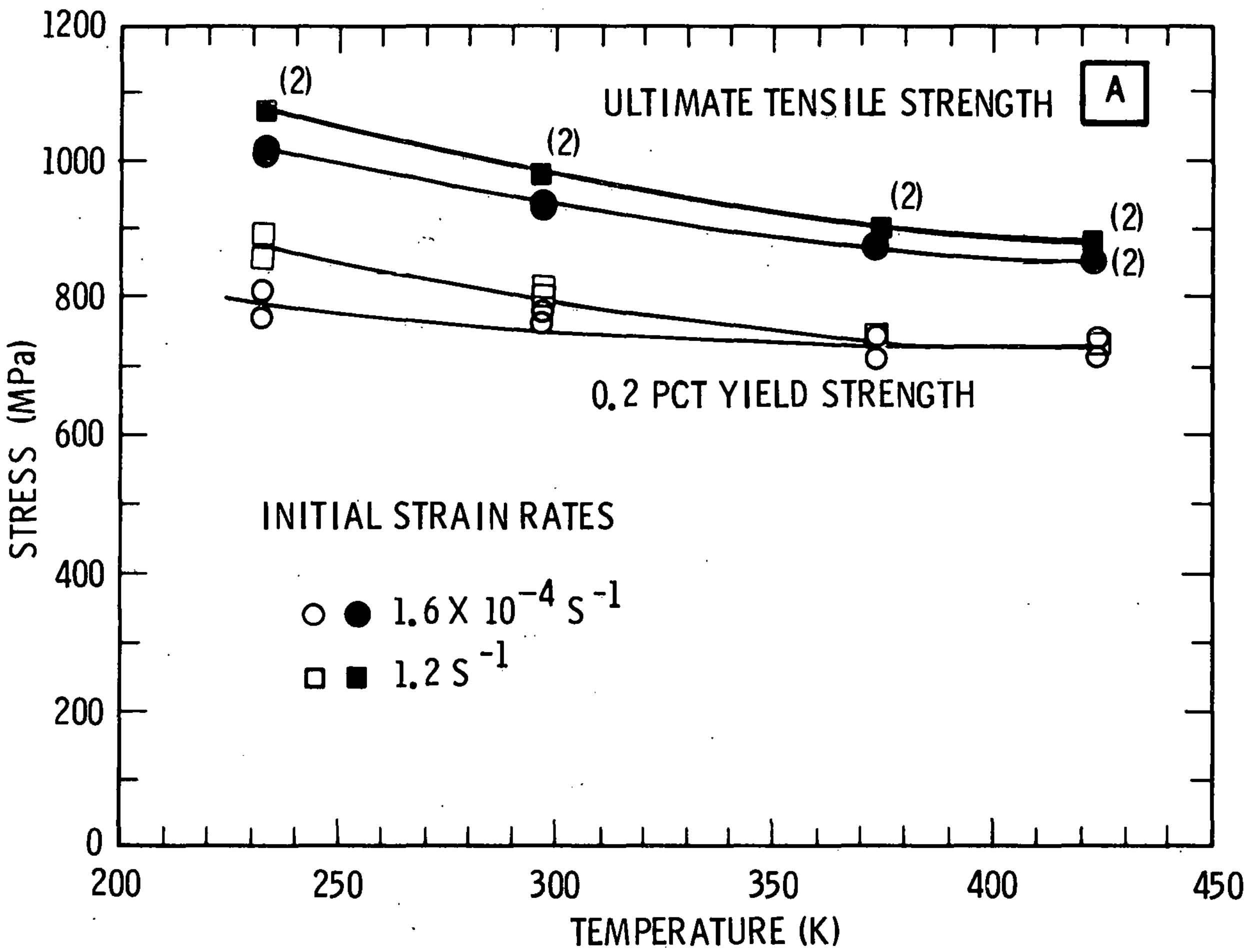

Figure 12. Influence of Test Temperature and Strain Rate on the Tensile Properties of Overaged Cast 17-4 PH Stainless Steel.

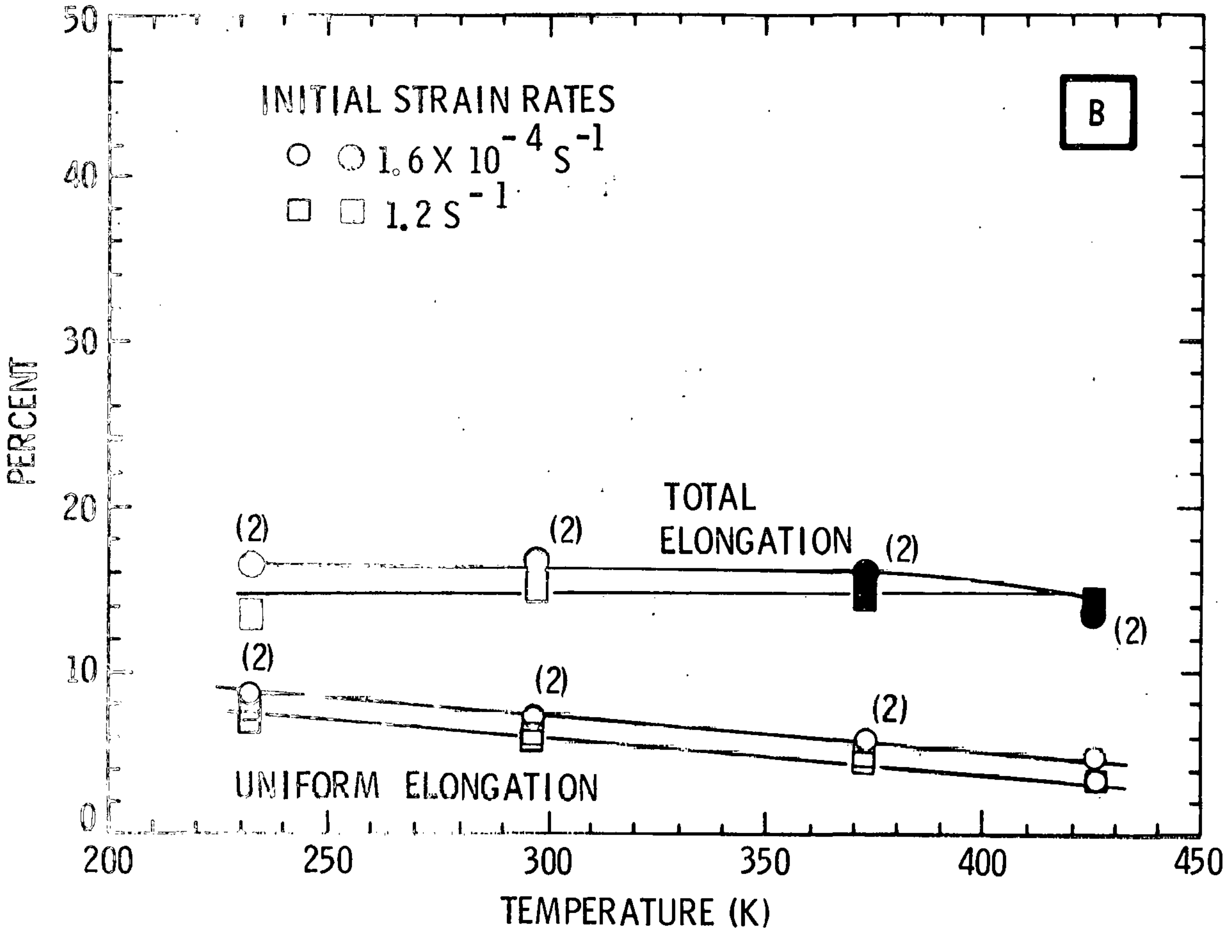

Figure 12. (Cont'd)

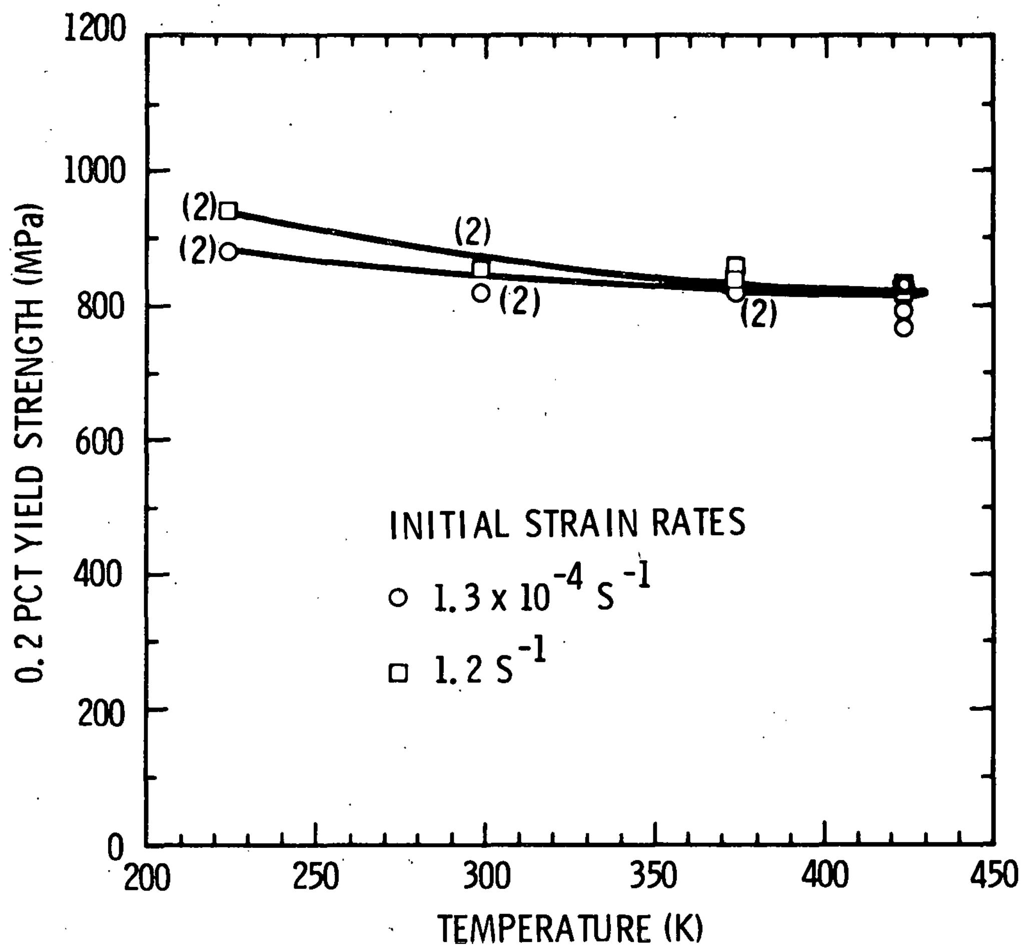

Figure 13. Influence of Test Temperature and Strain Rate on Compressive Yield Strength of Overaged Cast 17-4 PH Stainless Steel.

temperature and strain rate. Figure 12(b) shows that the uniform elongation decreased with both increasing test temperature and strain rate. This figure further indicates that, except at the lowest strain rate, $1.6 \times 10^{-4}\ s^{-1}$, and the highest test temperature, 433K, the total elongation was independent of test temperature and decreased with increasing strain rate. Finally, fractographic examination showed that the tensile failure mode was, in all cases, characterized by the formation of transgranular dimples, with the larger dimples being associated with various inclusions and δ-ferrite, Figure 14.

Classically, the fracture toughness behavior of low strength ferrous alloys has been examined by considering the influence of test temperature on the energy absorbed during impact fracture of a standard Charpy V-notch specimen. These investigations have typically shown that these steels undergo a tough-to-brittle transition with decreasing temperature, that is, there is a large reduction in absorbed energy over a relatively small temperature region. Figure 15 shows that the Charpy impact energy of the overaged 17-4 PH stainless steel casting presently under study also underwent such an energy related transition, although both the values of the upper shelf energy and rate of energy decrease with decreasing temperature were less than those normally reported for lower strength alloys (26). If a typical 20 joule absorbed energy tough-to-brittle transition temperature criteria were applied to overaged cast 17-4 PH, the T_{20J} transition temperature would have been approximately 350K, i.e., well above room temperature. Finally, comparison of the room temperature Charpy impact energy obtained for the overaged cast 17-4 PH ($E \sim 11$ joules) with that reported for wrought 17-4 PH aged at 866K (7) ($E \sim 37$ joules) suggests that cast 17-4 PH will absorb two-thirds less energy during impact loading than will wrought 17-4 Ph.

Although the dynamic fracture toughness measurements--as shown in Figure 16--also exhibited such a tough-to-brittle transition behavior,

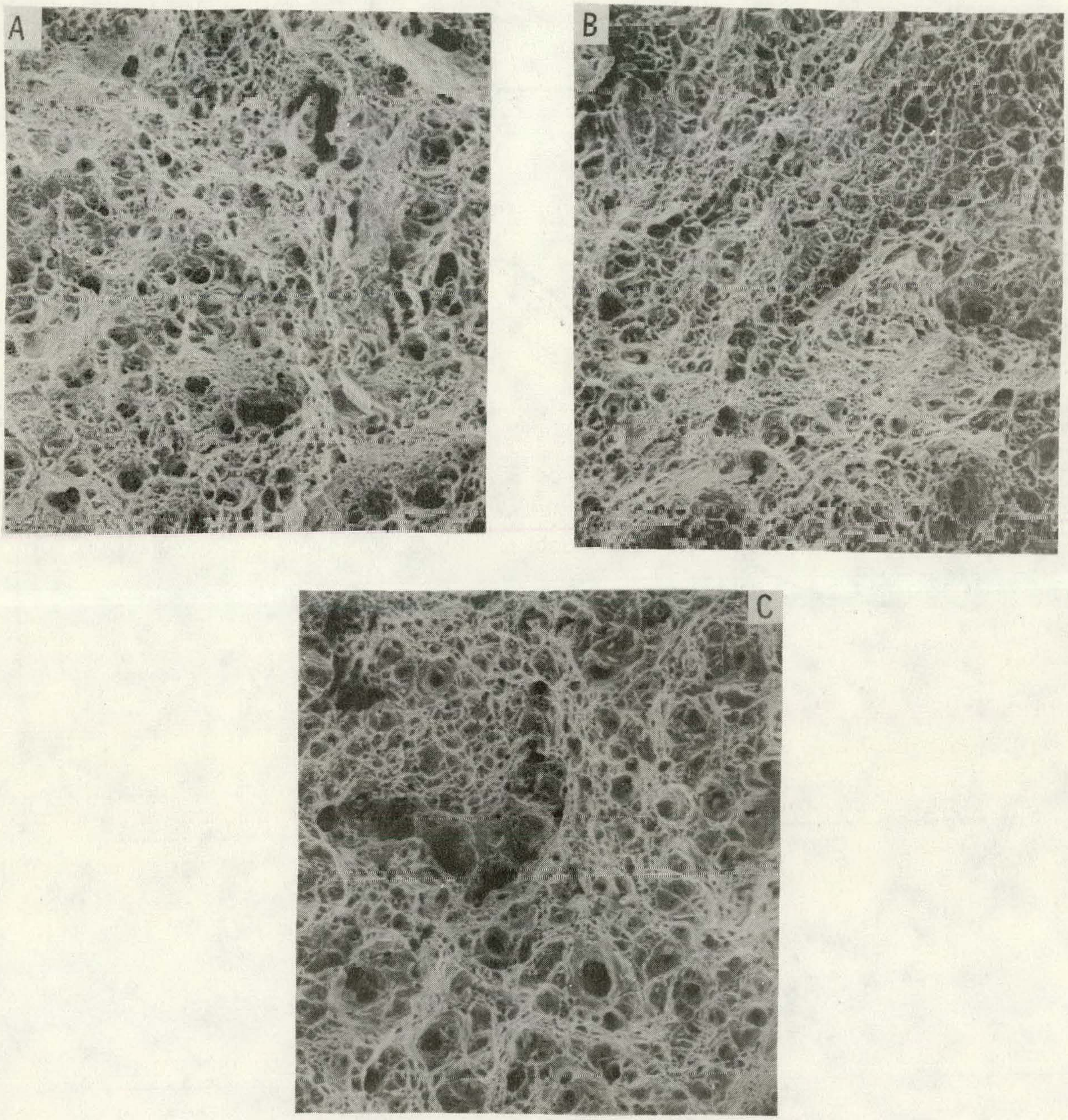

Figure 14. Scanning Electron Fractographs of Cast 17-4 PH Stainless Steel Tensile Samples Tested at:

(a) $\dot{\varepsilon} = 1.6 \times 10^{-4}\ s^{-1}$, $T = 233K$;

(b) $\dot{\varepsilon} = 1.6 \times 10^{-4}\ s^{-1}$, $T = 423K$; and

(c) $\dot{\varepsilon} = 1.2\ s^{-1}$, $T = 423K$.

Original Magnification: 400X.

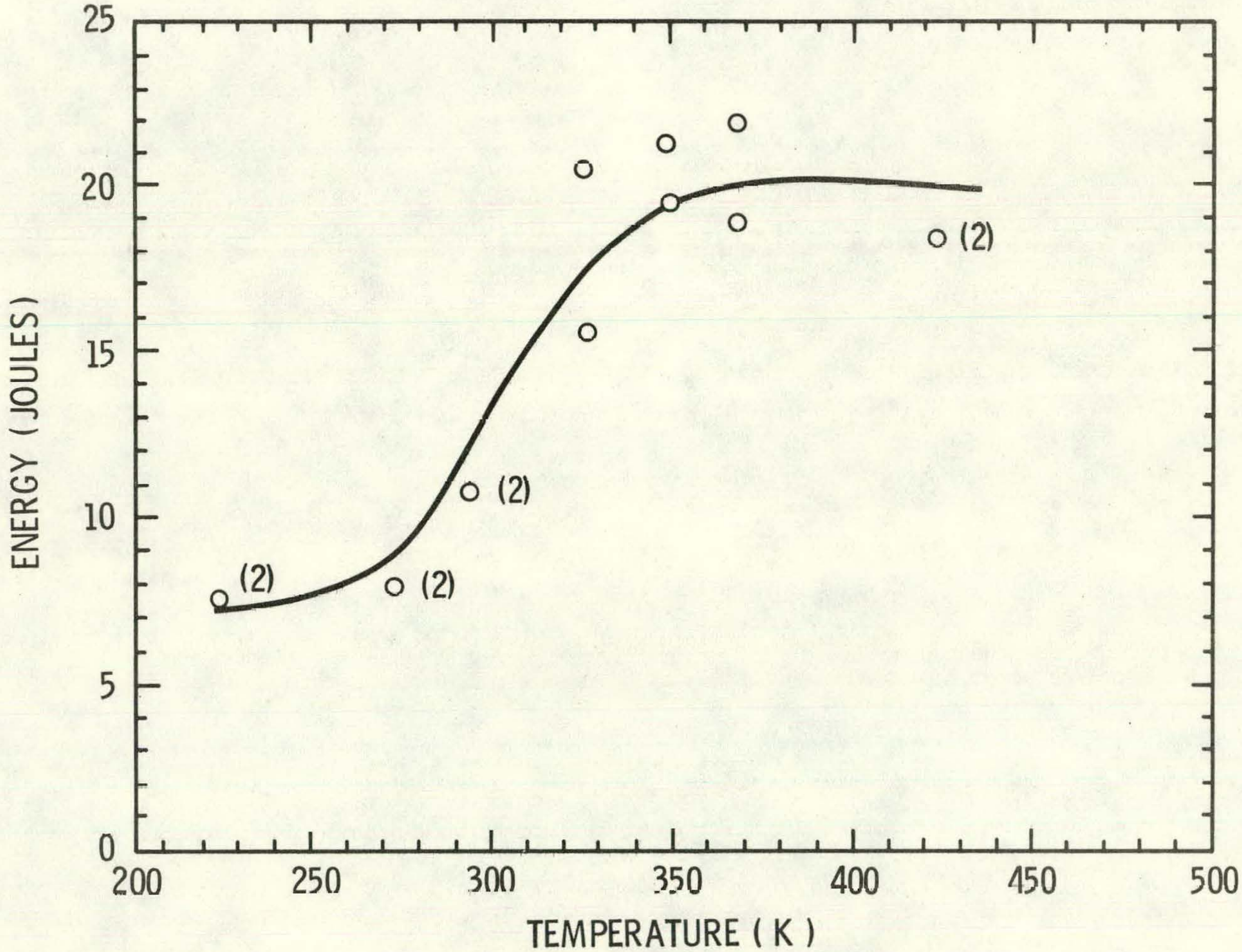

Figure 15. Charpy Impact Energy-Temperature Relationship in Cast 17-4 PH Stainless Steel.

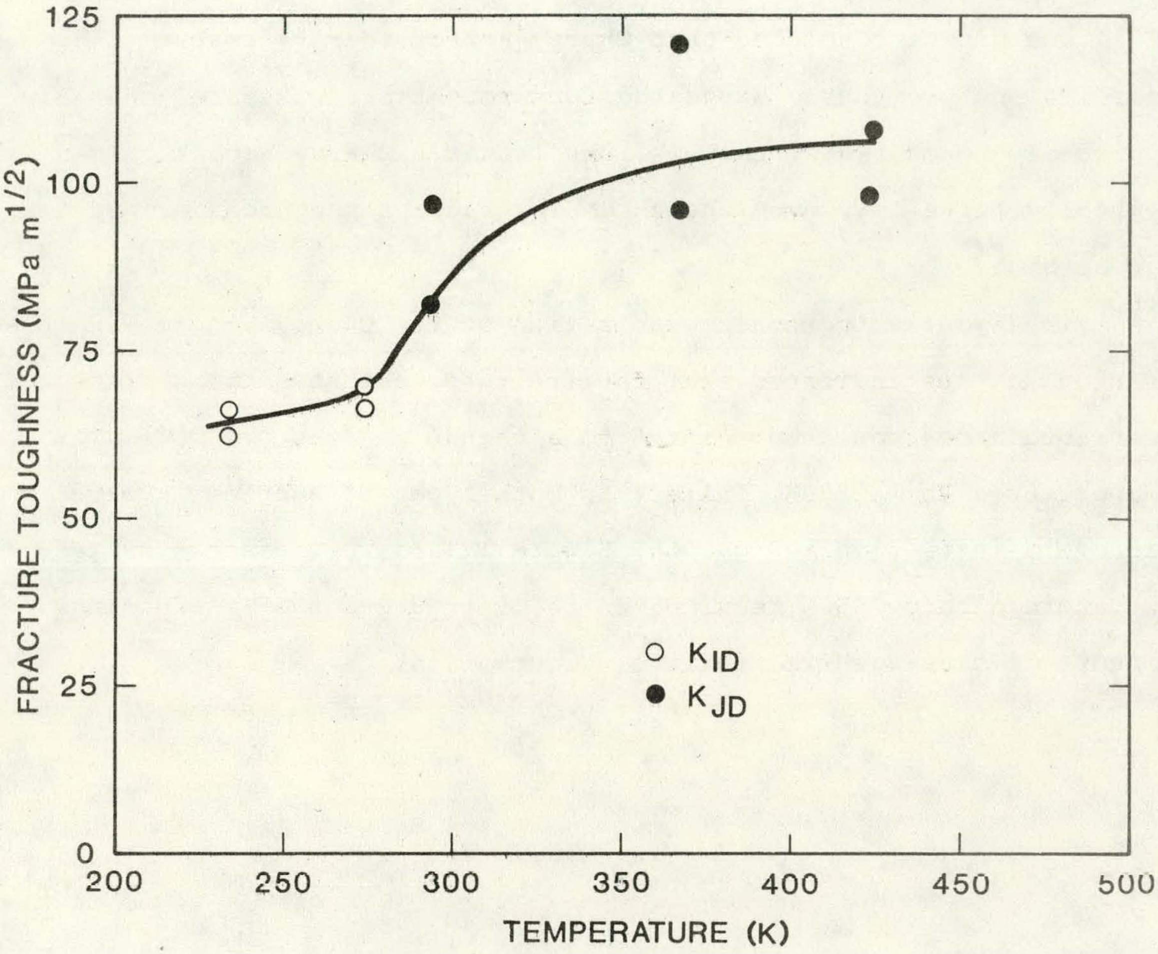

Figure 16. Dynamic Fracture Toughness-Temperature Relation in Cast 17-4 PH Stainless Steel.

the fracture toughness of the overaged 17-4 PH casting, even at the lowest test temperature examined, was still quite high, approximately 60 $MPam^{1/2}$. In addition, the room temperature toughness ($\sim$ 90 $MPam^{1/2}$) was at least comparable to that observed in wrought, overaged 17-4 PH (27), $K_{IC} \sim 130$ $MPam^{1/2}$. These observations reinforce those of Floreen (28), wherein he concluded that Charpy impact energy-fracture toughness correlations previously suggested for wrought products are generally not applicable to castings, that is, the latter's Charpy impact values are typically quite low, even though their fracture toughness properties may be high.

Finally, fractographic examination of the Charpy V-notch and pre-cracked samples indicated that the fracture toughness transitions described above could be related to a change in fracture mode. At temperatures above 350K, failure in both types of samples involved microvoid initiation and growth, Figure 17(a). Decreasing the test temperature below 350K resulted in the introduction of increasing amounts of cleavage-like failure, Figure 17(b).

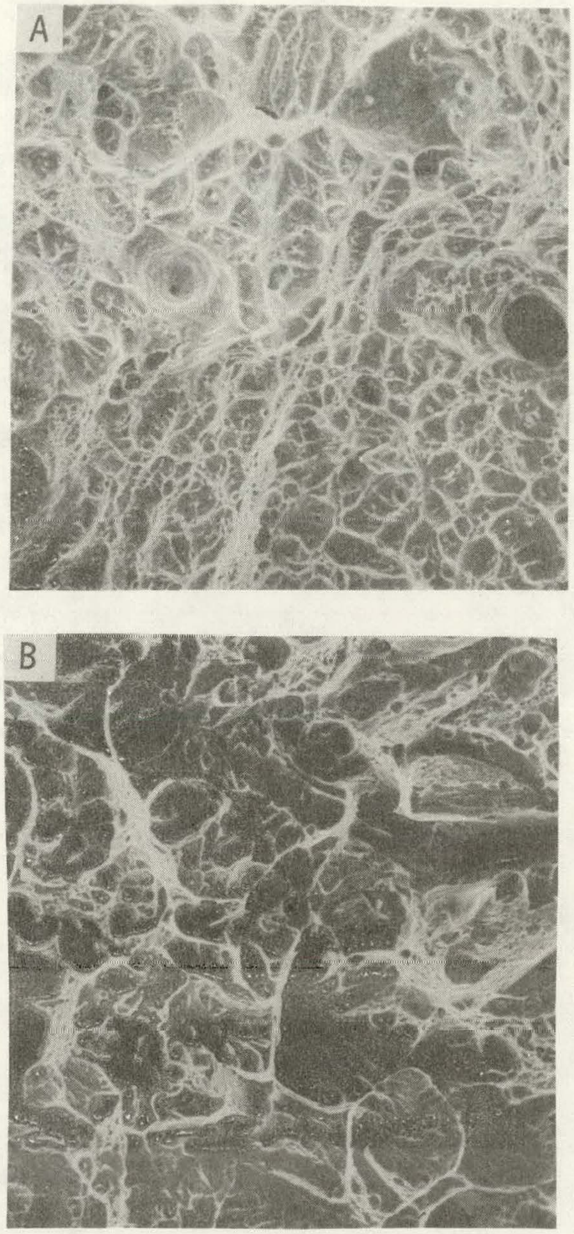

Figure 17. Scanning Electron Fractrographs of V-Notch Charpy Samples Tested at (a) 423K and (b) 233K. Original Magnification: 400X.

This Page Intentionally Left Blank.

SUMMARY AND CONCLUSIONS

This investigation has examined the physical and mechanical properties of an overaged 17-4 PH stainless steel casting and has compared these properties, where available, with those for wrought 17-4 PH stainless steel. The study has shown that--

a) The linear expansion behavior of cast 17-4 PH is identical to that of the wrought alloy.

b) The thermal properties, specific heat, thermal diffusivity and thermal conductivity, of cast 17-4 PH stainless steel are more sensitive to temperature than is wrought 17-4 PH, that is, they vary in a more complicated fashion with temperature than do the thermal properties of wrought 17-4 PH.

c) The elastic properties, Young's moduli and shear moduli, tend to be higher in cast 17-4 PH stainless steel than in the wrought alloy, although they both decrease with increasing temperature.

d) The tensile and compressive properties of cast 17-4 PH were to some degree a function of test temperature and strain rate, although not to the same degree as for lower strength ferrous steels.

e) The Charpy V-notch impact energy and the dynamic fracture toughness both exhibited a tough-to-brittle transition with decreasing test temperature. This transition was related to a change in fracture mode from ductile, dimple to cleavage-like.

f) While the Charpy impact energy for cast 17-4 PH was less than one-third that of wrought 17-4 PH, the dynamic fracture toughness of cast and wrought 17-4 PH were comparable. This reinforces previous suggestions that Charpy impact-fracture toughness correlations obtained for wrought products may not be applicable to castings.

REFERENCES

1. K. C. Antony, Aging Reactions in Precipitation Hardenable Stainless Steel, J. Metals, 15, 922 (1963).

2. E. Hornbogen and R. C. Glenn, A Metallographic Study of Precipitation of Cu from α Fe, Trans. Met. Soc. AIME, 218, 1064 (1960).

3. E. Hornbogen, Aging and Plastic Deformation of a Fe-0.9% Cu Alloy, Trans. ASM, 57, 120 (1964).

4. E. Hornbogen, The Role of Strain Energy During Precipitation of Cu and Au from α-Fe, Acta Met., 10, 525 (1962).

5. K. C. Russell and L. M. Brown, A Dispersion Strengthening Model Based on Differing Elastic Moduli Applied to the Fe-Cu System, Acta Met., 20, 969 (1972).

6. A. Youle and B. Ralph, A Study of the Precipitation of Cu from α-Fe in the Pre-Peak to Peak Hardness Range of Aging, Met. Sci. Jn., 6, 149 (1972).

7. H. J. Rack and David Kalish, The Strength, Fracture Toughness and Low Cycle Fatigue Behavior of 17-4 PH Stainless Steel, Met. Trans., 5, 1595 (1974).

8. G. N. Goller and N. C. Clarke, Jr., New Precipitation-Hardening Stainless Steels, Iron Age, 165, 86 (1950).

9. K. J. Irvine, D. T. Llewellyn and F. B. Pickering, Controlled-Transformation Stainless Steels, J. Iron Steel Inst., 192, 218 (1959).

10. C. S. Carter, D. G. Farwick, A. M. Ron and J. M. Ucheda, Stress Corrosion Properties of High Strength, Precipitation Hardening Stainless Steel, Corrosion, 27, 190 (1971).

11. E. A. Lauchner, The Microstructure and Ductility of 17-4 PH and 15-5 PH Stainless Steels, J. Material, 5, 129 (1970).

12. Memo, J. E. McCreight to H. J. Rack, November 28, 1979, subject: Thermal Expansion Measurements.

13. R. E. Taylor and H. Groot, Thermophysical Properties of Alloys, TPRL 195, Thermophysical Properties Research Laboratory, Purdue University, West Lafayette, Indiana, August 1979.

14. J. F. Gieske, Ultrasonic Measurement of Elastic Moduli of 17-4 PH Stainless Steel and U-2 wt. pt M_O from -40° to 800°C, SAND80-1121, July 1980.

15. J. M. Krafft and R. A. Gray, "Effects of Neutron Irradiation on Bulk and Micro Flow-Fracture Behavior of Pressure Vessel Steels," in Practical Applications of Fracture Mechanics to Pressure Vessel Technology, Institution of Mechanical Engineers, London, 1971, pp. 93-102.

16. R. A. Wullaert, Applications of the Instrumented Charpy Impact Test, Impact Testing of Metals ASTM STP 466, Am. Soc. Testing and Materials, Philadelphia, PA, 1970, pp. 148-164.

17. W. L. Server and A. S. Tetelman, The Use of Pre-Cracked Charpy Specimens to Determine Dynamic Fracture Toughness, Eng. Fract. Mech., 4, 367 (1972).

18. W. L. Server, Impact Three-Point Bend Testing for Notched and Precracked Specimens, Jn. Testing and Evaluation, 6, 29 (1978).

19. V. Arp, J. H. Wilson, L. Winrich and P. Sikora, Thermal Expansion of Some Engineering Materials from 20 to 293K, Cryogenics, 2, 230 (1962).

20. A. F. Hoenie and D. B. Roach, New Developments in High-Strength Stainless Steels, U. S. Air Force Report DMIC-223, 1966.

21. I. B. Fieldhouse and J. I. Lang, Measurement of Thermal Properties, U. S. Air Force Report WADD-TR-60-904, 1961.

22. O. L. Deel and H. Mindlin, Engineering Data on New Aerospace Structural Materials, AFML-TR-72-196, Vol. 1, Battelle Columbus Labs, September 1972.

23. Anon, Armco 17-4 PH Precipitation-Hardening Stainless Steel Bar and Wire, Armco Steel Corp., S-6C, LA 10273, January, 1974.

24. E. G. Takacs, Armco 17-4 PH, Type 410 - Young's Modulus and Poisson's Ratio, Adv. Mat'ls Div., Armco Steel Corp., October 1976.

25. W. J. Lanning, Torsion Properties of 17-4 PH and 15-5 PH Stainless Steel Bars, Advanced Mat'ls Div., Armco Steel Corp., March 1972.

26. J. F. Knott, Mechanics and Mechanism of Large-Scale Brittle Fracture in Structural Metals, Mat. Sci. Eng., 7, 1 (1971).

27. H. J. Rack, Unpublished Research, Sandia Laboratories, Albuquerque, NM, 87185, April 1975.

28. S. Floreen, The Fracture Toughness of Cast High-Strength Steels, Jn. Eng. Mat. Tech., 99, 70 (1977).

This Page Intentionally Left Blank.

APPENDIX A

Mechanical Property Sample Configurations*

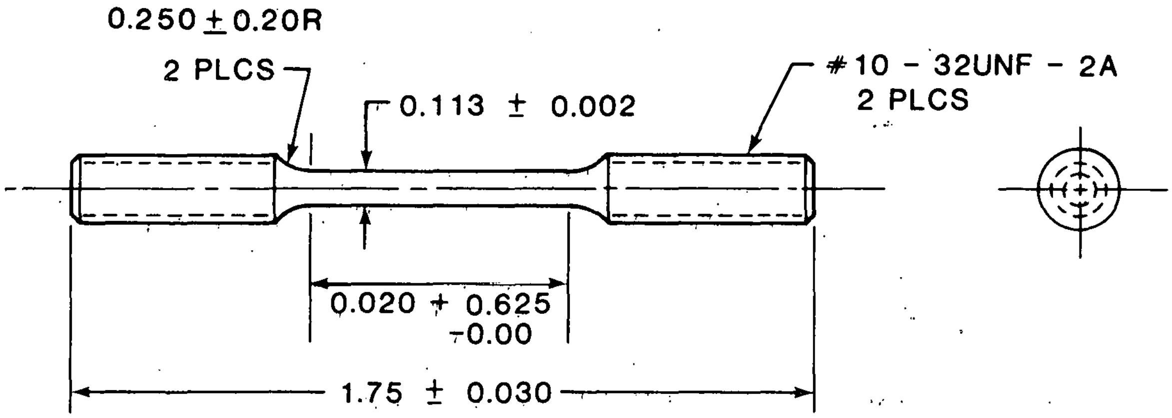

Figure A-1. Subsized Tensile Specimen.

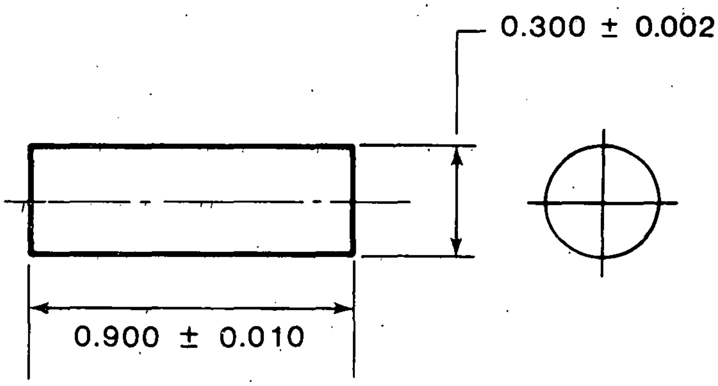

Figure A-2. Cylindrical Compression Specimen.

*All dimensions in inches.

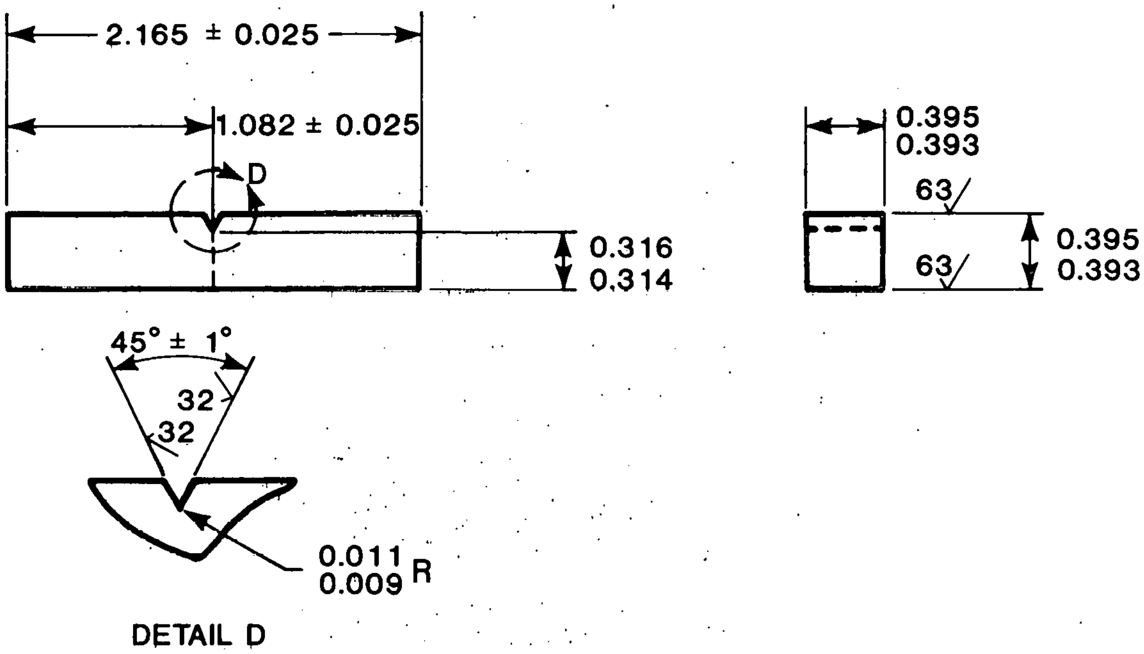

Figure A-3. ASTM Standard Charpy Impact Specimen.

APPENDIX B

Representative Tensile Stress-Strain Curves for Overaged 17-4 PH Stainless Steel Casting

Figure	Test Temperature (K)	Strain Rate (Δ^{-1})
B-A	233	1.6×10^{-4}
B-B	233	1.2
B-C	297	1.6×10^{-4}
B-D	297	1.2
B-E	433	1.6×10^{-4}
B-F	433	1.2

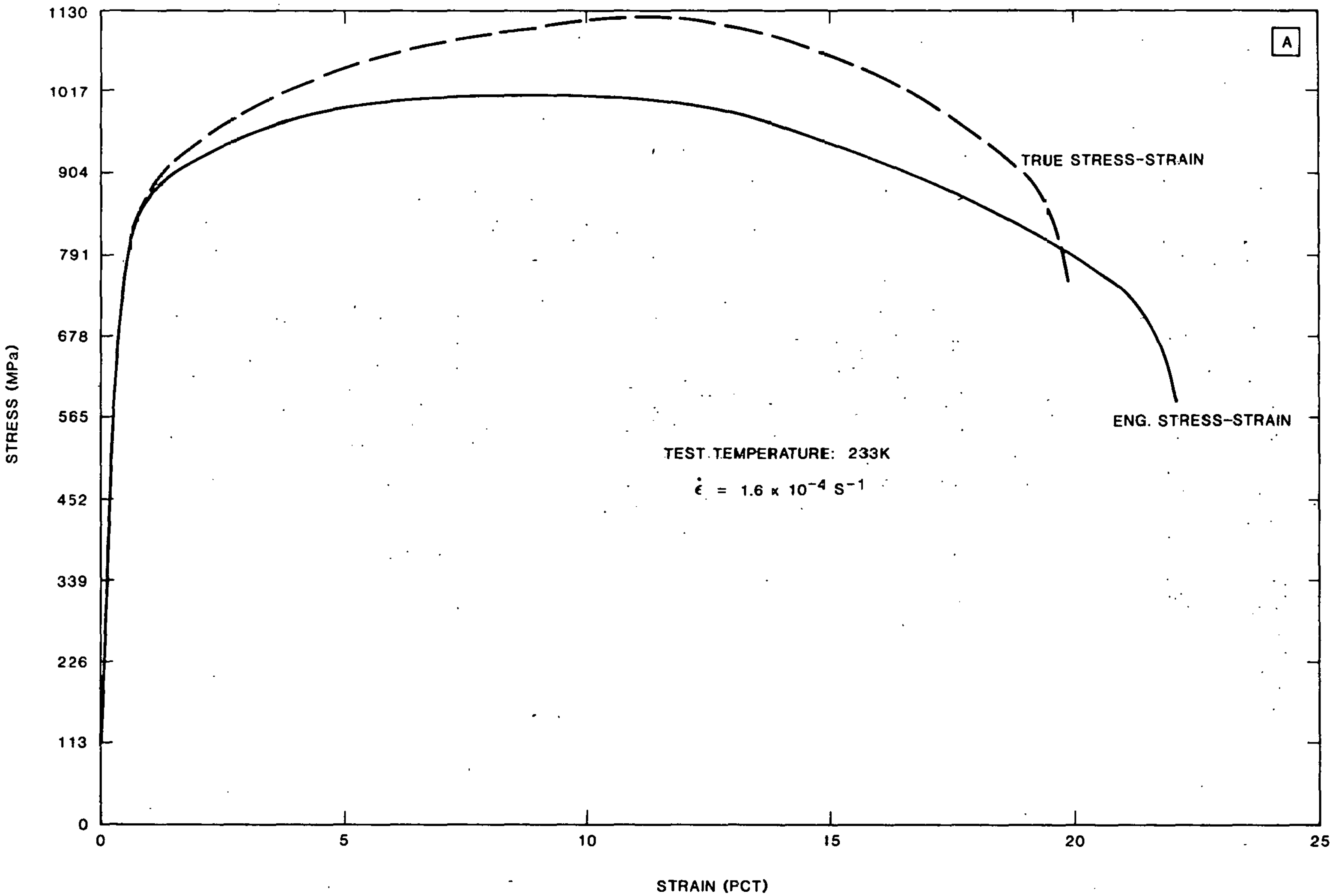
A
TRUE STRESS-STRAIN
ENG. STRESS-STRAIN
TEST TEMPERATURE: 233K
$\dot{\epsilon}$ = 1.6 x 10^{-4} S^{-1}
STRESS (MPa)
1130
1017
904
791
678
565
452
339
226
113
0
STRAIN (PCT)
0
5
10
15
20
25

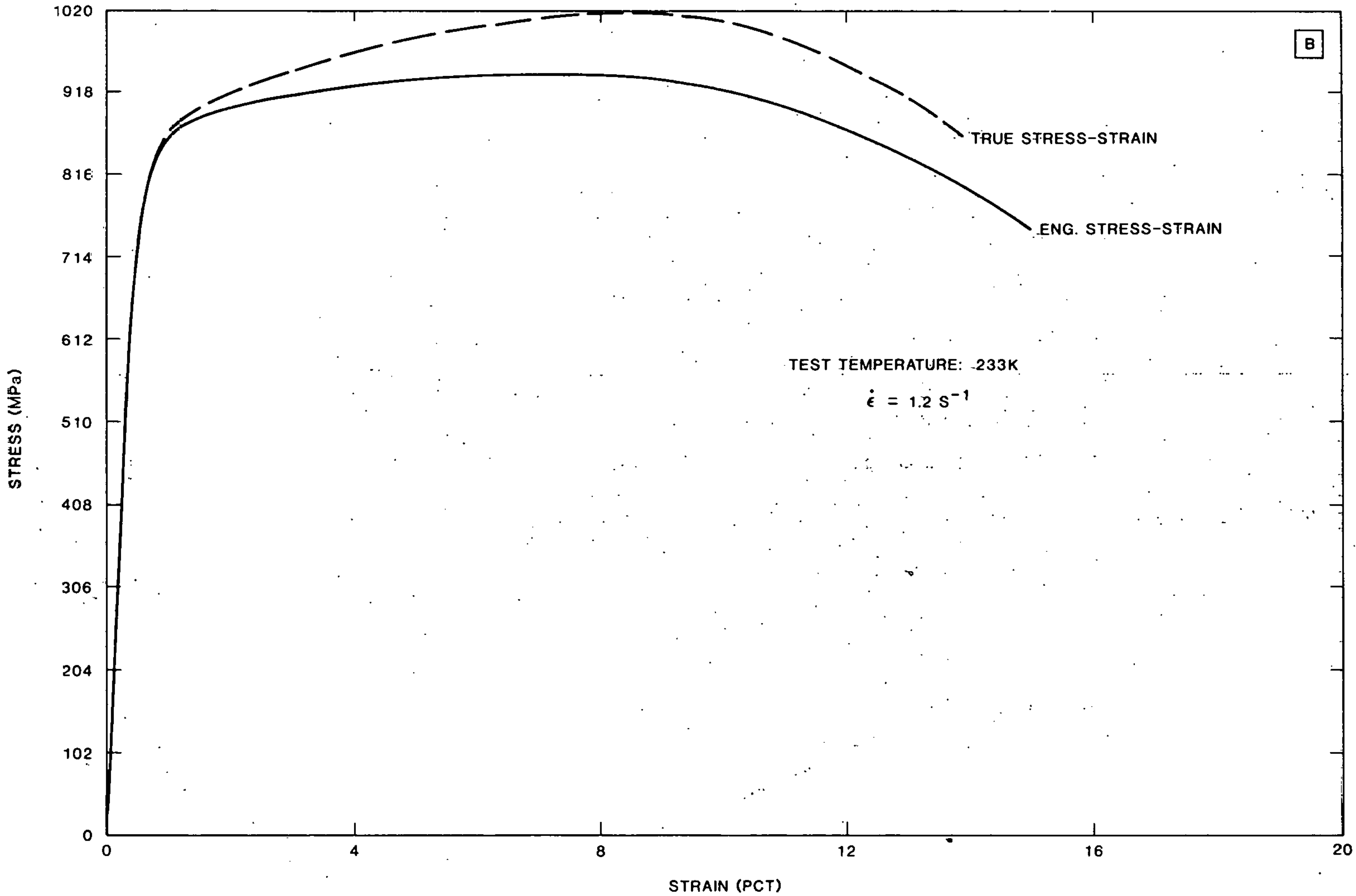
B
STRESS (MPa)
1020
918
816
714
612
510
408
306
204
102
0
STRAIN (PCT)
0
4
8
12
16
20
TRUE STRESS-STRAIN
ENG. STRESS-STRAIN
TEST TEMPERATURE: 233K
$\dot{\epsilon}$ = 1.2 S^{-1}

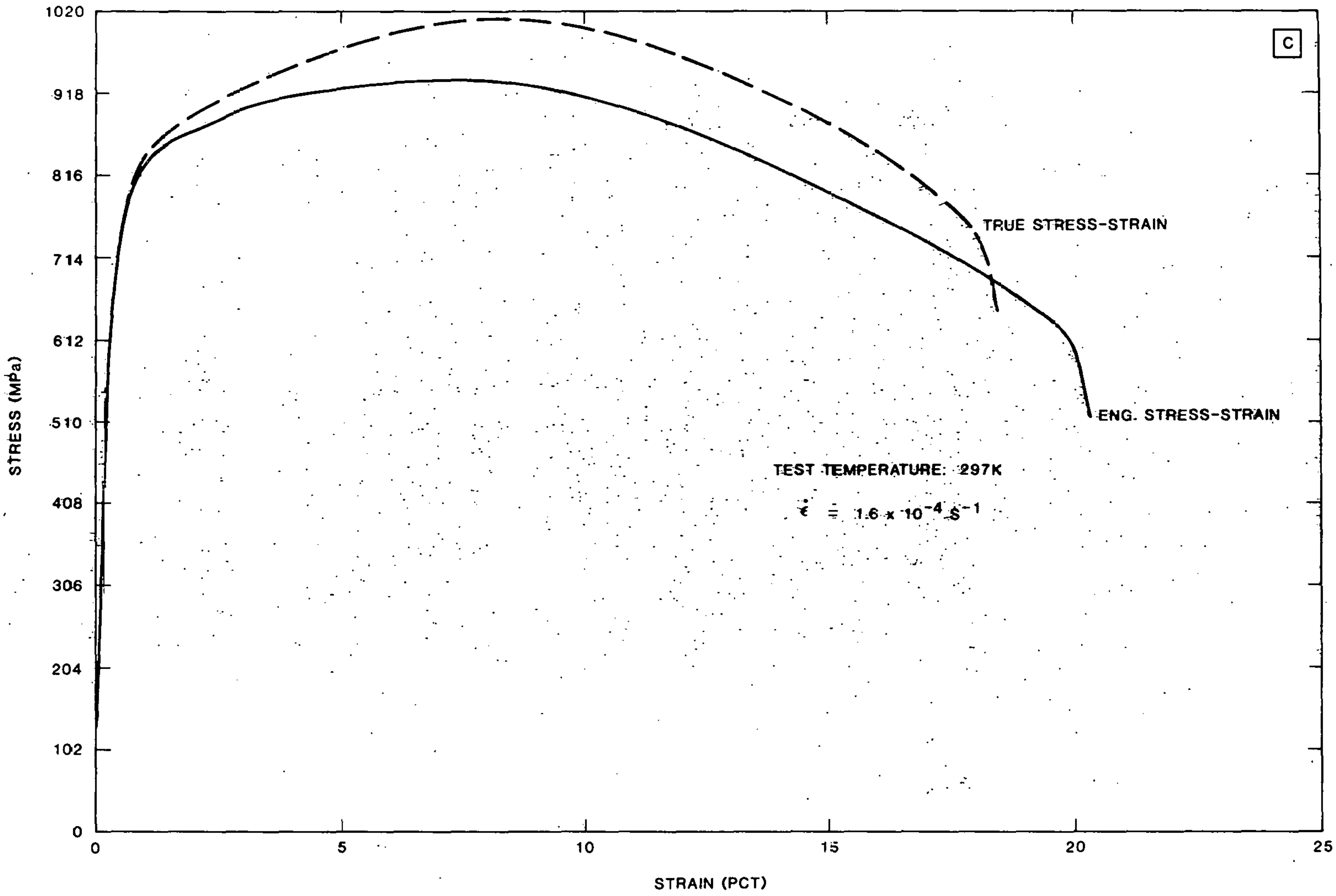

C
STRESS (MPa)
1020
918
816
714
612
510
408
306
204
102
0
STRAIN (PCT)
0
5
10
15
20
25
TRUE STRESS-STRAIN
ENG. STRESS-STRAIN
TEST TEMPERATURE: 297K
$\dot{\epsilon}$ = 1.6 x 10^{-4} S^{-1}

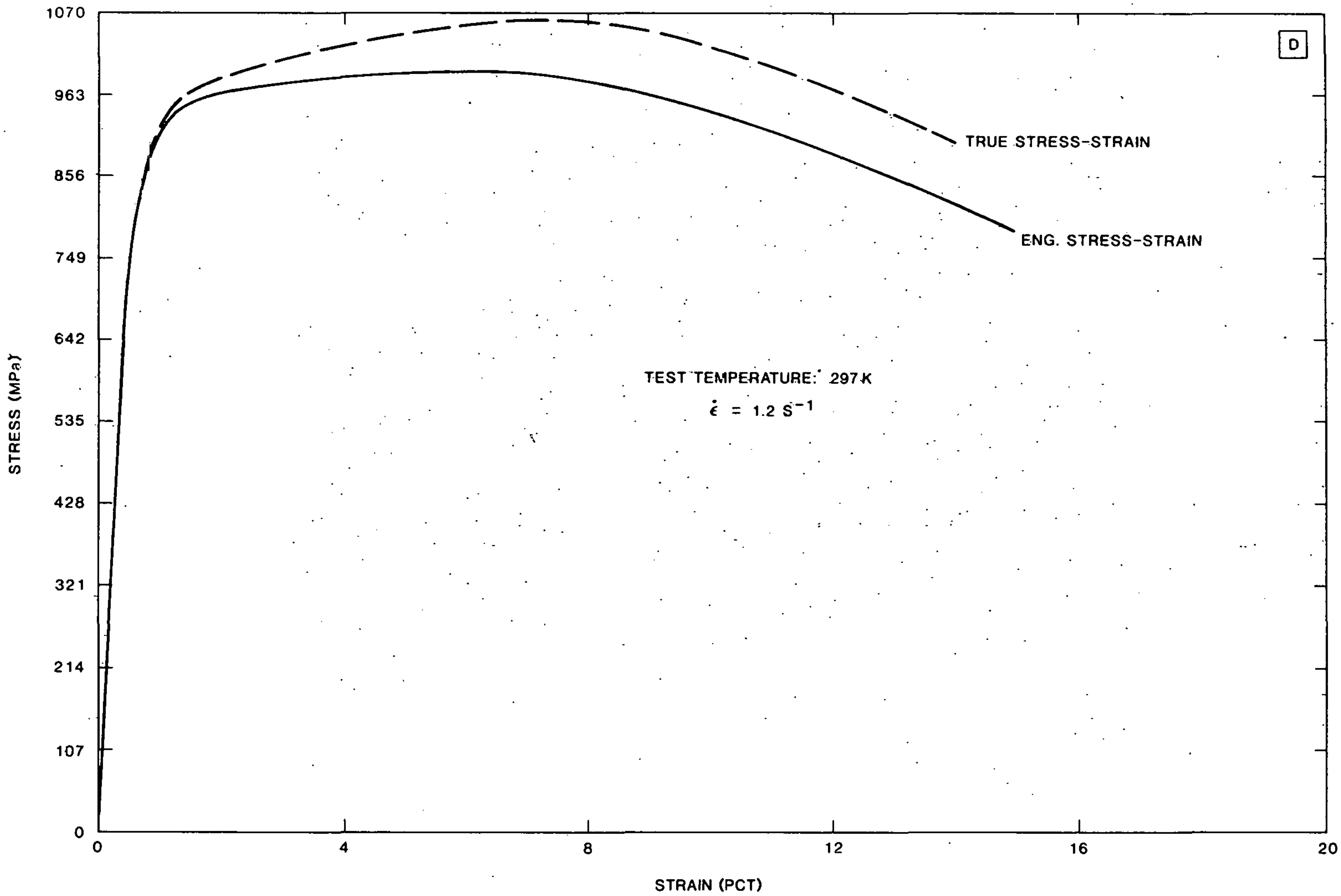
1070
963
856
749
642
535
428
321
214
107
0
STRESS (MPa)
0
4
8
12
16
20
STRAIN (PCT)
D
TRUE STRESS-STRAIN
ENG. STRESS-STRAIN
TEST TEMPERATURE: 297 K
$\dot{\epsilon}$ = 1.2 S^{-1}

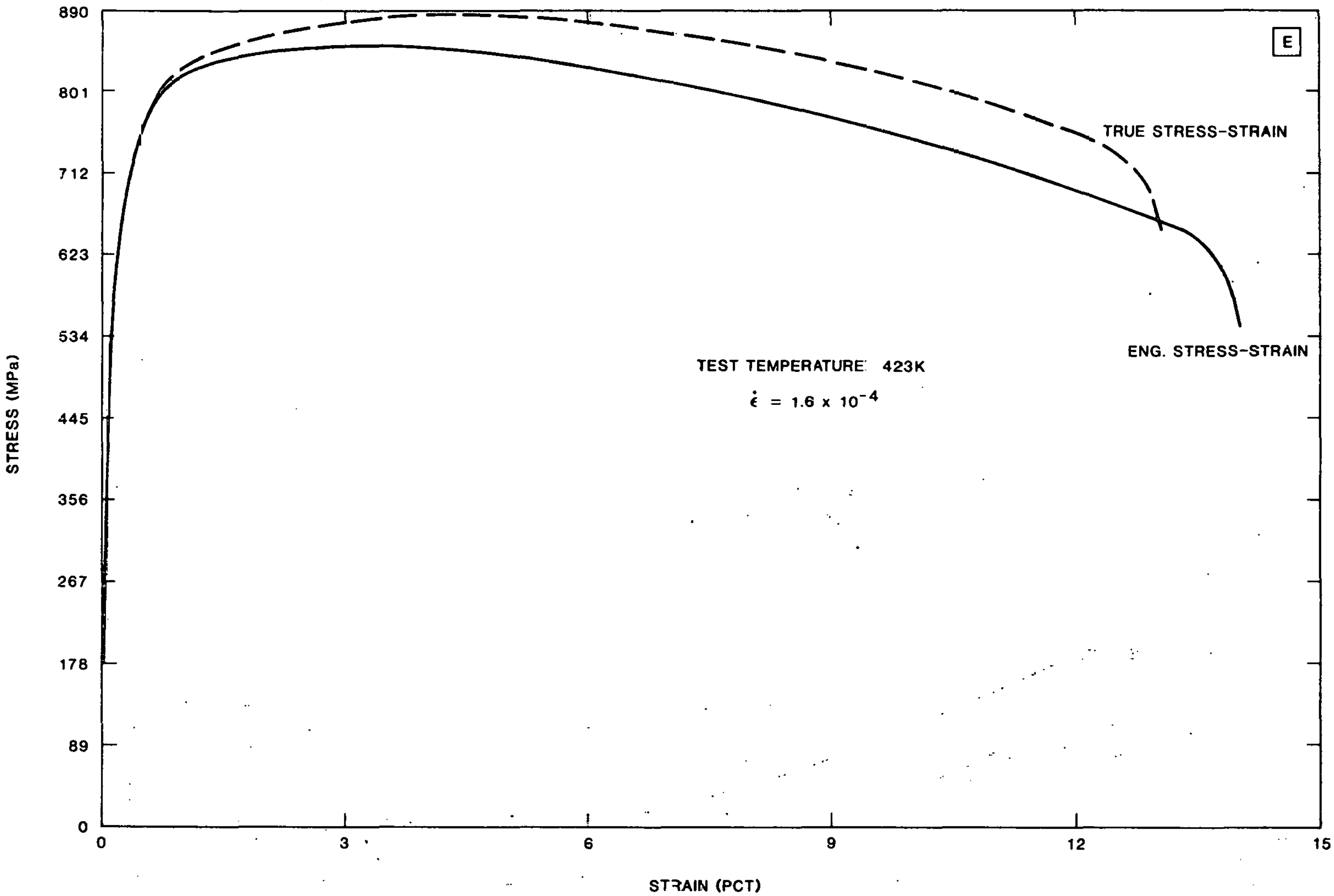

E
TRUE STRESS-STRAIN
ENG. STRESS-STRAIN
TEST TEMPERATURE: 423K
$\dot{\epsilon}$ = 1.6 x 10^{-4}
STRESS (MPa)
890
801
712
623
534
445
356
267
178
89
0
0
3
6
9
12
15
STRAIN (PCT)

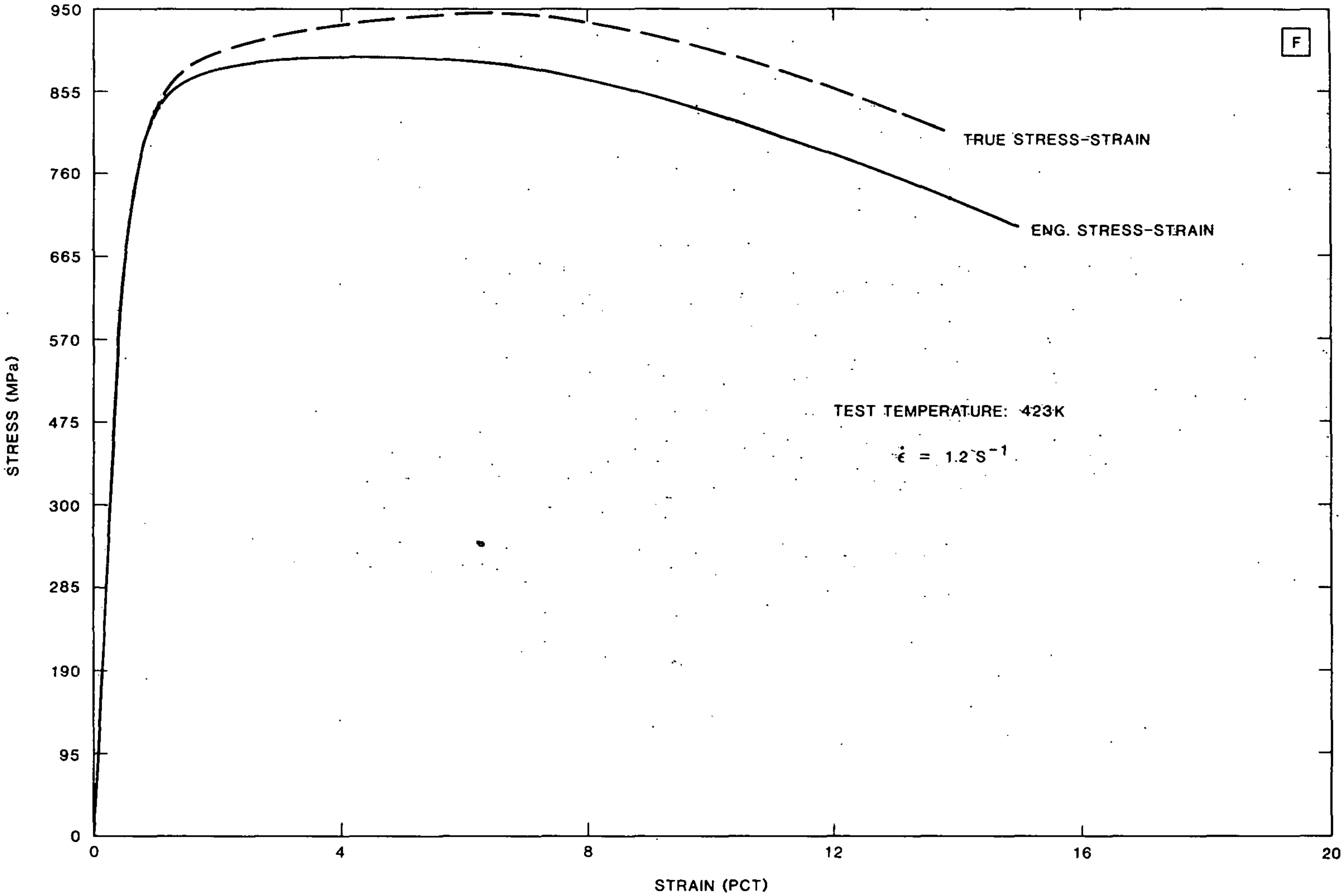
F
TRUE STRESS-STRAIN
ENG. STRESS-STRAIN
TEST TEMPERATURE: 423K
$\dot{\epsilon} = 1.2 \ S^{-1}$
STRESS (MPa)
950
855
760
665
570
475
300
285
190
95
0
STRAIN (PCT)
0
4
8
12
16
20

This Page Intentionally Left Blank.

APPENDIX C

Representative Compressive Stress-Strain Curves for Overaged 17-4 PH Stainless Steel Casting

Figure	Test Temperature (K)	Strain Rate (s^{-1})
C-A	233	1.3×10^{-4}
C-B	233	1.2
C-C	297	1.3×10^{-4}
C-D	297	1.3
C-E	433	1.3×10^{-4}
C-F	433	1.3

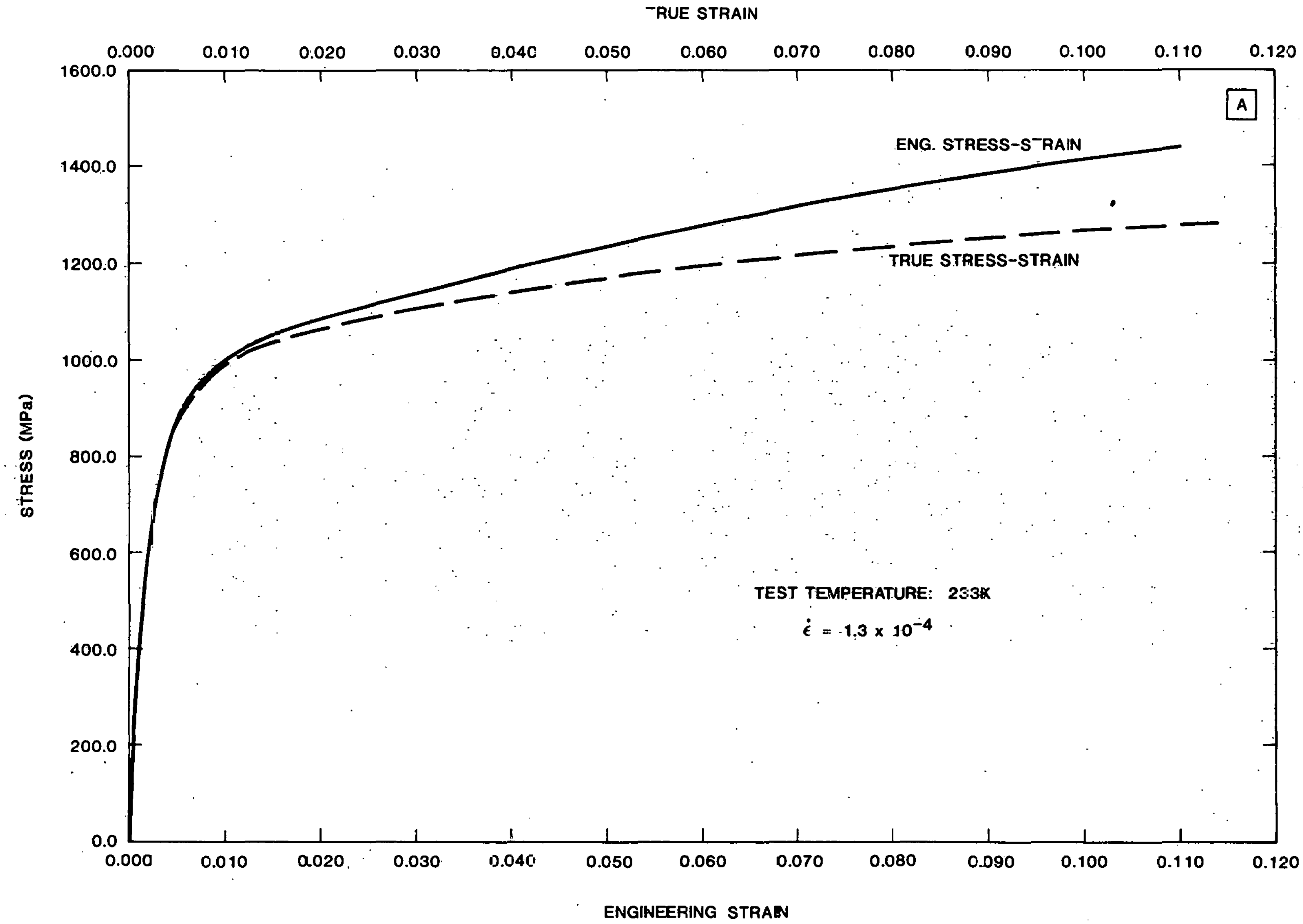
TRUE STRAIN
0.000
0.010
0.020
0.030
0.040
0.050
0.060
0.070
0.080
0.090
0.100
0.110
0.120
A
ENG. STRESS-STRAIN
TRUE STRESS-STRAIN
STRESS (MPa)
1600.0
1400.0
1200.0
1000.0
800.0
600.0
400.0
200.0
0.0
TEST TEMPERATURE: 233K
$\dot{\epsilon}$ = 1.3 x 10^{-4}
ENGINEERING STRAIN

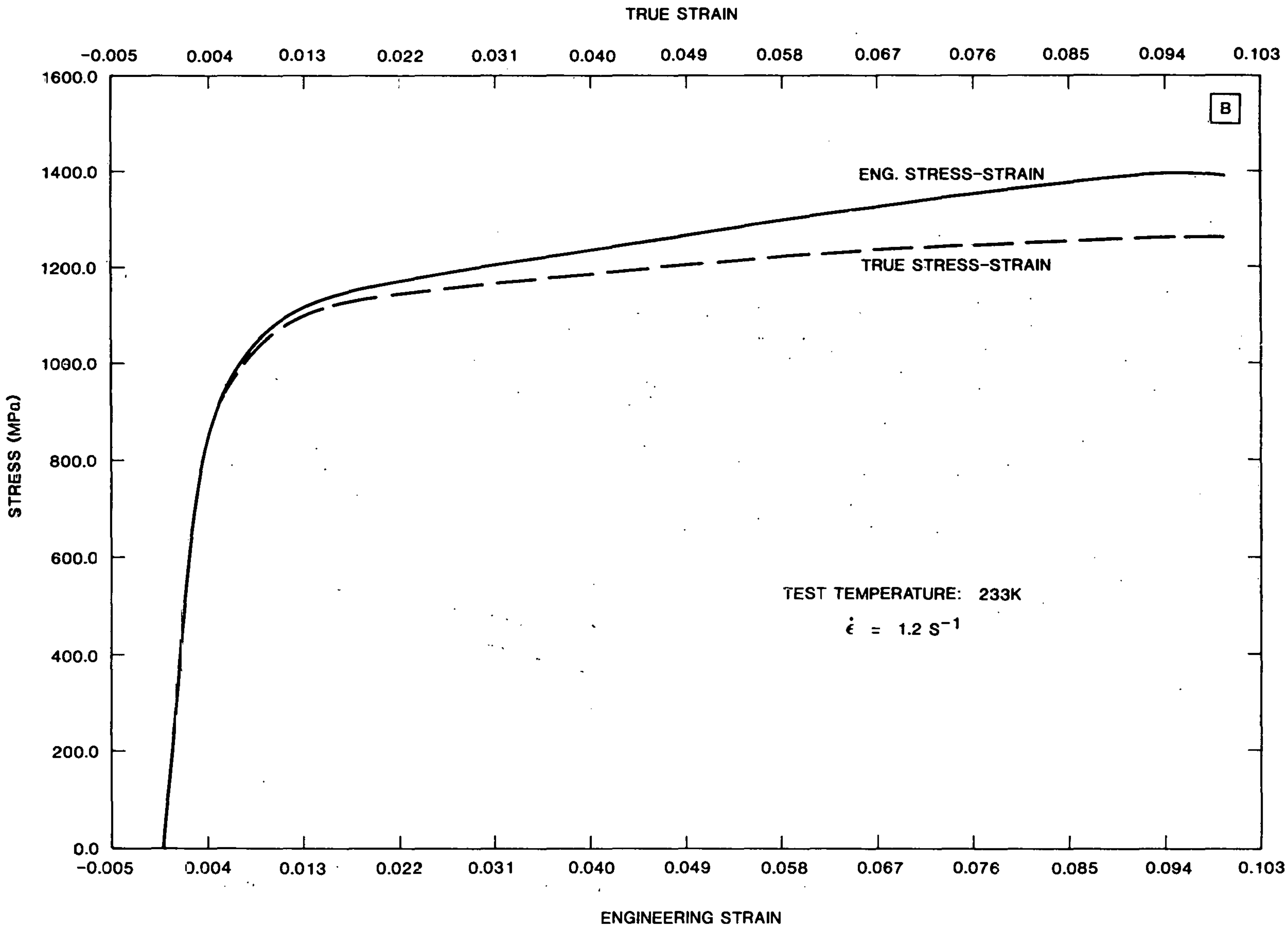
TRUE STRAIN
-0.005
0.004
0.013
0.022
0.031
0.040
0.049
0.058
0.067
0.076
0.085
0.094
0.103
B
ENG. STRESS-STRAIN
TRUE STRESS-STRAIN
STRESS (MPa)
1600.0
1400.0
1200.0
1000.0
800.0
600.0
400.0
200.0
0.0
TEST TEMPERATURE: 233K
$\dot{\epsilon}$ = 1.2 S^{-1}
-0.005
0.004
0.013
0.022
0.031
0.040
0.049
0.058
0.067
0.076
0.085
0.094
0.103
ENGINEERING STRAIN

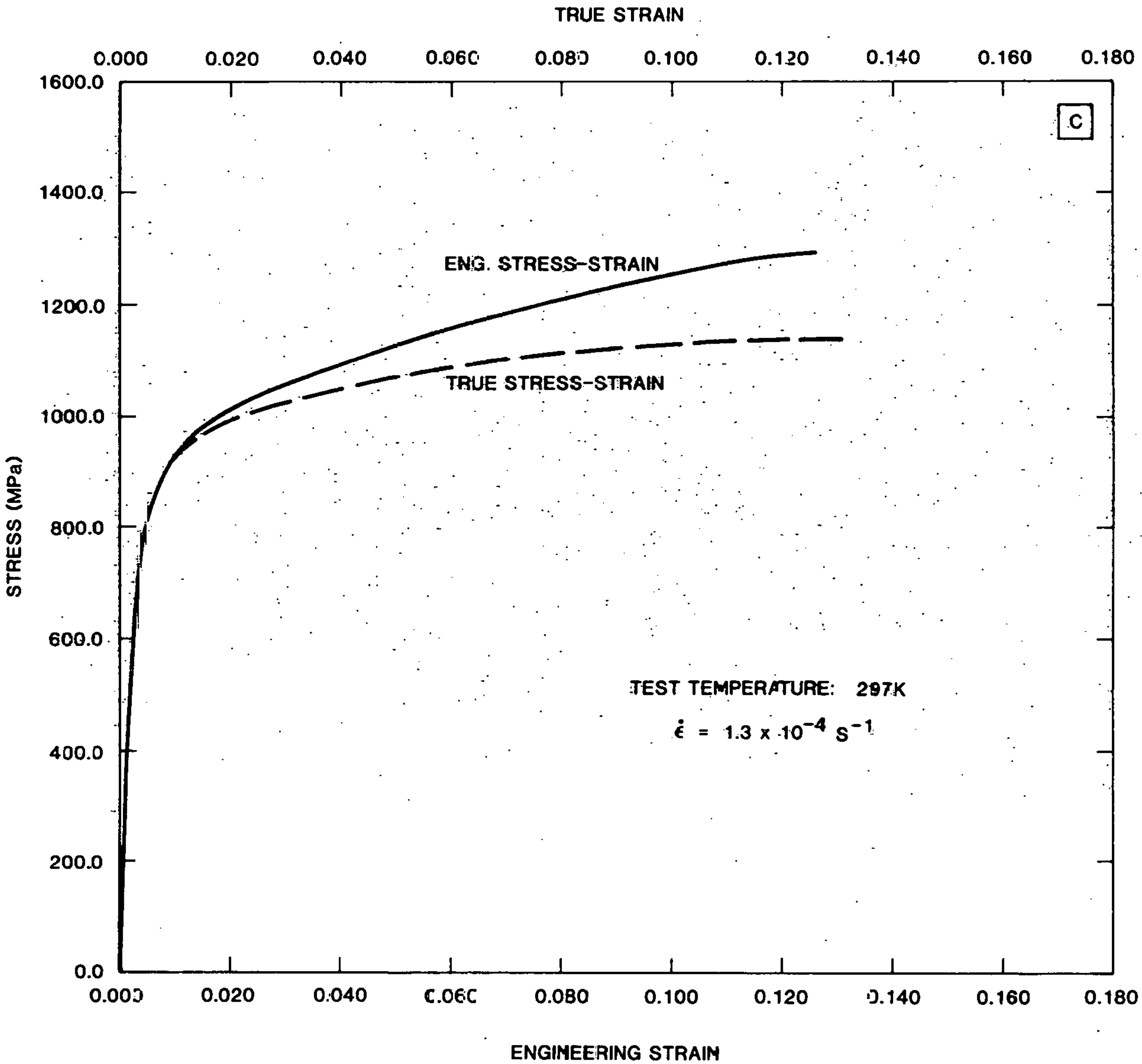
TRUE STRAIN
0.000
0.020
0.040
0.060
0.080
0.100
0.120
0.140
0.160
0.180
C
ENG. STRESS-STRAIN
TRUE STRESS-STRAIN
STRESS (MPa)
1600.0
1400.0
1200.0
1000.0
800.0
600.0
400.0
200.0
0.0
TEST TEMPERATURE: 297K
$\dot{\epsilon}$ = 1.3 x 10^{-4} S^{-1}
0.000
0.020
0.040
0.060
0.080
0.100
0.120
0.140
0.160
0.180
ENGINEERING STRAIN

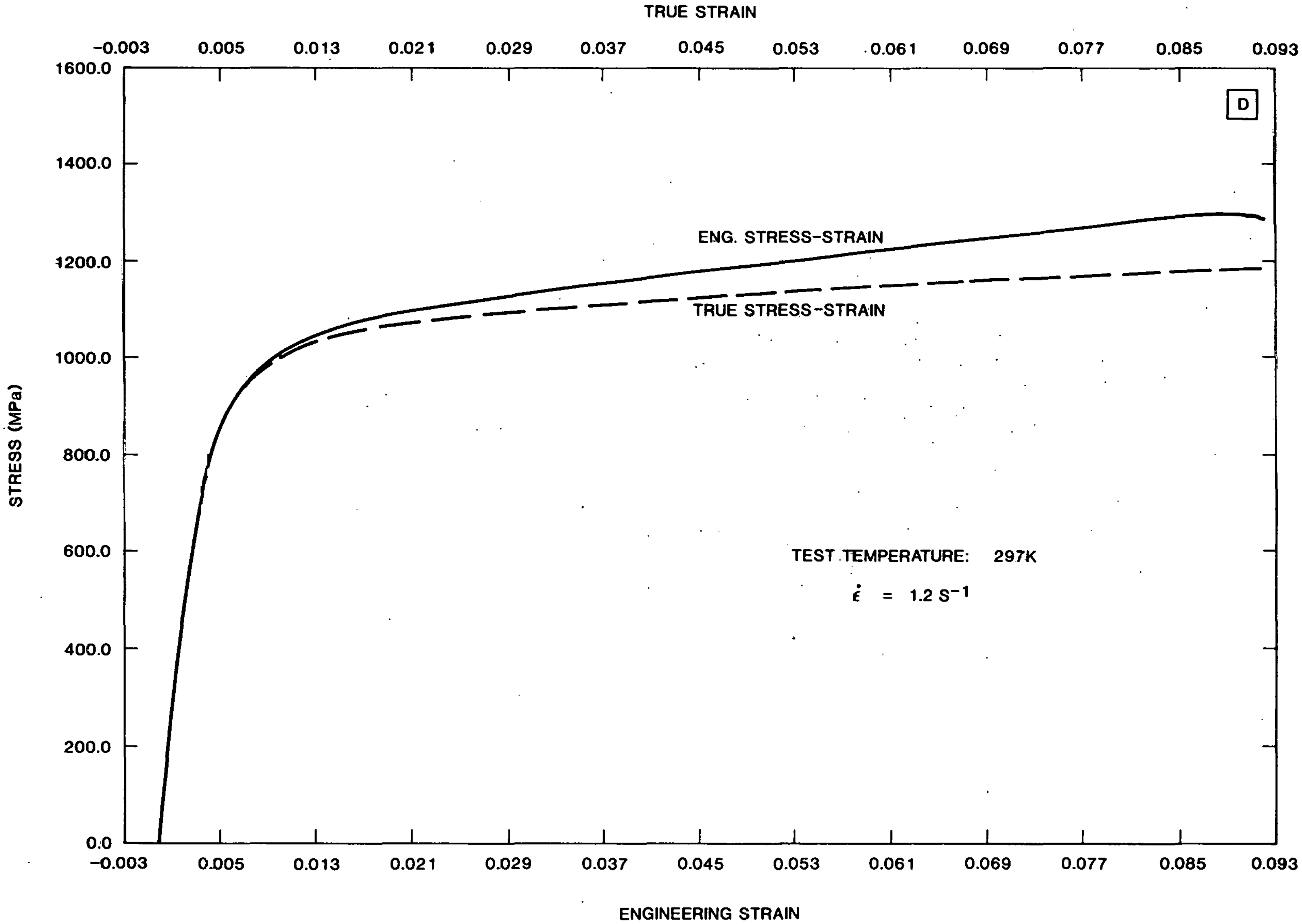
TRUE STRAIN
-0.003
0.005
0.013
0.021
0.029
0.037
0.045
0.053
0.061
0.069
0.077
0.085
0.093
1600.0
1400.0
1200.0
1000.0
800.0
600.0
400.0
200.0
0.0
STRESS (MPa)
D
ENG. STRESS-STRAIN
TRUE STRESS-STRAIN
TEST TEMPERATURE: 297K
$\dot{\epsilon}$ = 1.2 S^{-1}
ENGINEERING STRAIN

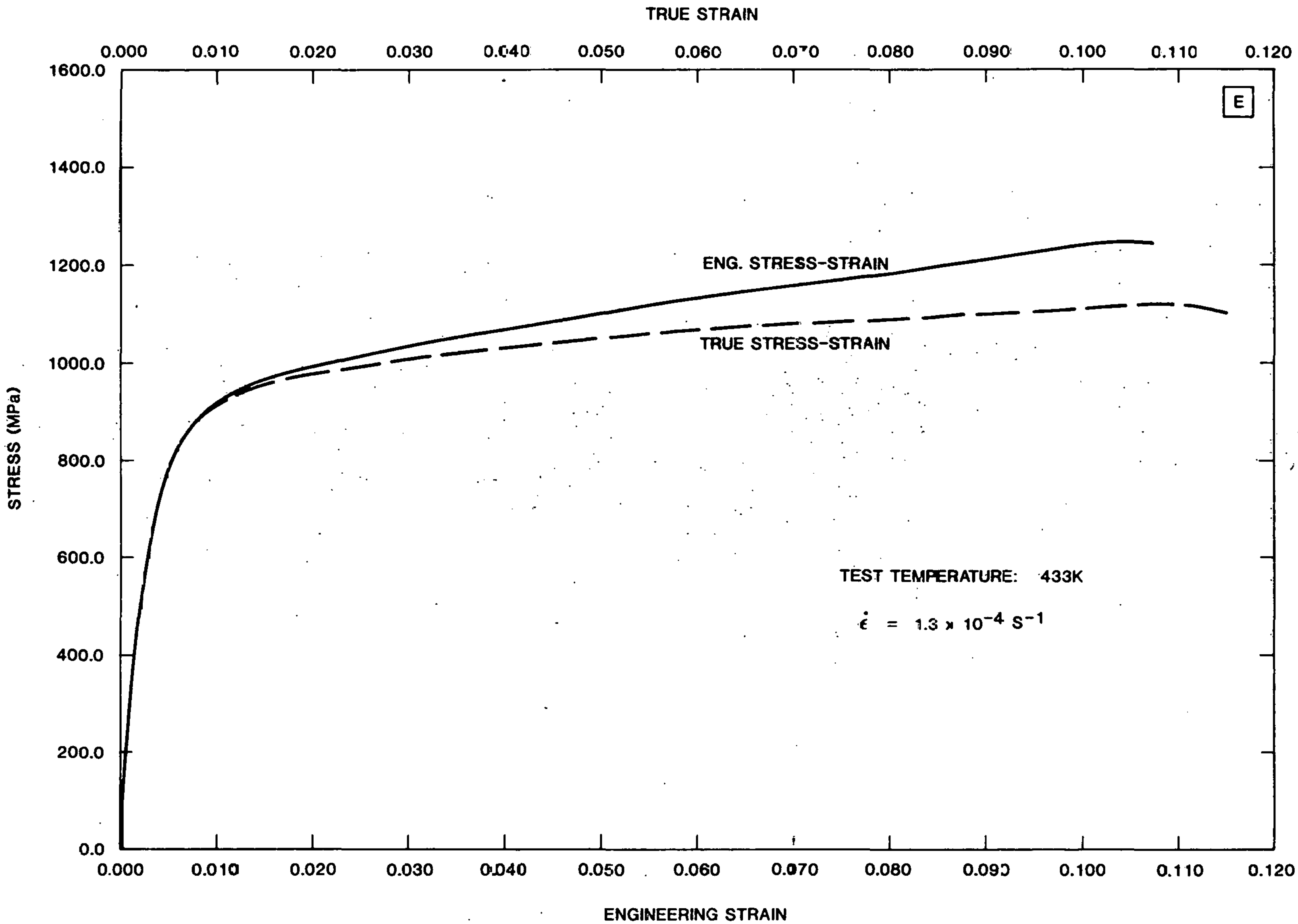
TRUE STRAIN
0.000 0.010 0.020 0.030 0.040 0.050 0.060 0.070 0.080 0.090 0.100 0.110 0.120
E
STRESS (MPa)
0.0 200.0 400.0 600.0 800.0 1000.0 1200.0 1400.0 1600.0
ENG. STRESS-STRAIN
TRUE STRESS-STRAIN
TEST TEMPERATURE: 433K
$\dot{\epsilon} = 1.3 \times 10^{-4}\ S^{-1}$
0.000 0.010 0.020 0.030 0.040 0.050 0.060 0.070 0.080 0.090 0.100 0.110 0.120
ENGINEERING STRAIN

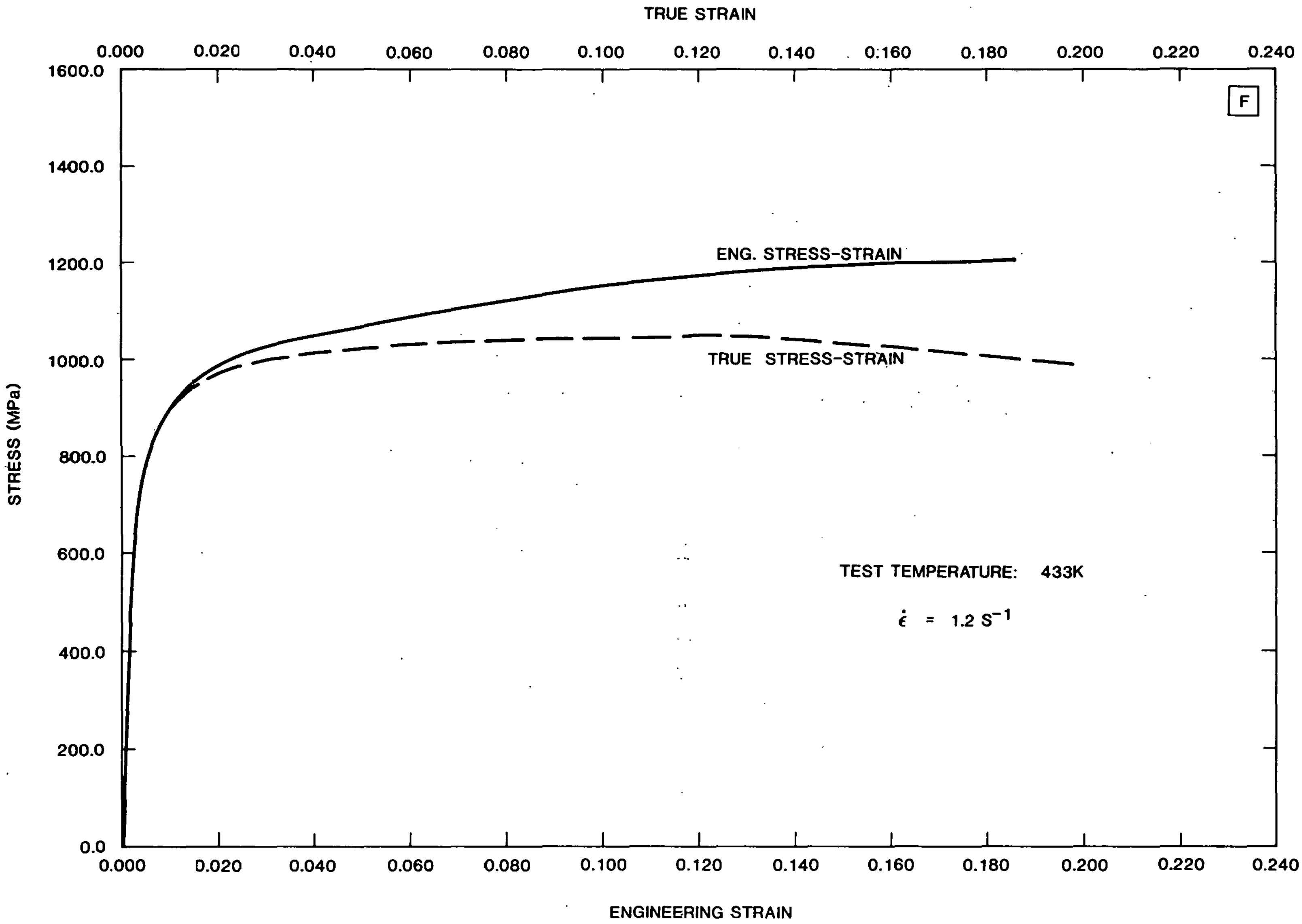
TRUE STRAIN
0.000
0.020
0.040
0.060
0.080
0.100
0.120
0.140
0.160
0.180
0.200
0.220
0.240
1600.0
1400.0
1200.0
1000.0
800.0
600.0
400.0
200.0
0.0
STRESS (MPa)
F
ENG. STRESS-STRAIN
TRUE STRESS-STRAIN
TEST TEMPERATURE: 433K
$\dot{\epsilon}$ = 1.2 S^{-1}
ENGINEERING STRAIN

This Page Intentionally Left Blank.

Unlimited Release
DISTRIBUTION:

U. S. Department of Energy
Technical Information Center
Attn: DOE/TIC-4500-R67

Allied-General Nuclear Services
P. O. Box 847
Barnwell, SC 29812
Attn: P. Highberger

Battelle Columbus Laboratories
Office of Nuclear Waste Isolation
505 King Avenue
Columbus, OH 43201
Attn: R. Peterson

Battelle Memorial Institute
Pacific Northwest Laboratory
P. O. Box 999
Richland, WA 99352
Attn: R. E. Rhoads

E. I. du Pont de Nemours & Co.
Savannah River Plant
Aiken, SC 29801
Attn: S. Petrie

Electric Power Research Institute
P. O. Box 10412
Palo Alto, CA 94304
Attn: C. Chan

Exxon Nuclear Co., Inc.
777 106th Avenue NE
Bellevue, WA 98004
Attn: J. H. Nordahl

General Atomic Company
P. O. Box 81608
San Diego, CA 92138
Attn: R. M. Burgoyne

General Electric Company
175 Curtner Avenue
San Jose, CA 95125
Attn: C. Davis

Hanford Engineering Development Lab
P. O. Box 1970
Richland, WA 99352
Attn: P. R. Clements

Lawrence Livermore Lab (1)
P. O. Box 808
Livermore, CA 94550
Attn: K. C. MacMillan, L-333
R. T. Langland, L-90

Nuclear Assurance Corporation
24 Executive Park West
Atlanta, GA 30329
Attn: C. Johnson

Nuclear Packaging, Inc.
1733 South Fawcett
Tacoma, WA 98402
Attn: J. D. Simchuk

Oak Ridge National Laboratory
P. O. Box X
Oak Ridge, TN 37830
Attn: L. B. Shappert

J. L. Ridihalgh, President
Ridihalgh & Associates
2122 Iuka Avenue
Columbus, OH 43201

Rockwell International (1)
Atomics International Division
Rocky Flats Plant
P. O. Box 464
Golden, CO 80401
Attn: R. W. Skulski
W. D. Stump
B. Cross

Southwest Research Institute
P. O. Drawer 28510
San Antonio, TX 78228
Attn: R. A. Baker

Stearns-Roger, Inc.
P. O. Box 5888
Denver, CO 80217
Attn: W. H. Brinkman

Transnuclear, Inc.
One North Broadway
White Plains, NY 10601
Attn: L. Macklin

U. S. Department of Energy (6)
Advanced Nuclear System
MS B107
Washington, D. C. 20545
Attn: F. Dieringer
S. Meyers
M. J. Lawrence
R. B. Chitwood
R. Staker
F. Falci

Unlimited Release
Distribution (continued):

U. S. Department of Energy (3)
Albuquerque Operations Office
P. O. Box 5400
Albuquerque, NM 87185
Attn: E. C. Hardin, Jr.
R. Y. Lowrey
K. Carlson

U. S. Department of Energy
FFTF Project Office
P. O. Box 550
Richland, WA 99352
Attn: John Patterson

U. S. Department of Energy
Office of Military
Division of Research, Development and Testing
Washington, D. C. 20545
Attn: Paul O. Mathews, Research Branch

Applied Science and Technology
16630 Sagewood Lane
Poway, CA
Attn: R. E. Nickell

U. S. Department of Transportation
MTB (DMT-221)
Room 6518, Buzzards Point Building
400 Seventh St. SW
Washington, D. C. 20590
Attn: R. Rawl

U. S. Nuclear Regulatory (3) Commission
Washington, D. C. 20555
Attn: W. R. Lahs
C. E. MacDonald
D. R. Hopkins

Westinghouse Electric Corp.
P. O. Box W
Oak Ridge, TN 37830
Attn: J. E. Rutenber

1725 J. A. Andersen
4400 A. W. Snyder
Attn: 4410 D. J. McCloskey
4420 J. V. Walker
4450 J. A. Reuscher
4440 G. R. Otey
Attn: 4441 M. Berman
4443 D. A. Dahlgren
4442 W. A. Von Riesemann
4442 E. P. Chen

4500 E. H. Beckner
Attn: 4510 W. D. Weart
4530 R. W. Lynch
4540 M. L. Kramm
4550 R. M. Jefferson
4551 R. E. Luna
4551 R. P. Sandoval
4552 R. B. Pope (15)
4552 G. C. Allen, Jr.
4552 T. A. Duffey
4552 R. G. Eakes (5)
4552 G. H. Lamoreaux
4552 B. J. Joseph
4552 W. B. Leisher
4552 L. E. Romesberg
4552 S. H. Sutherland
4552 A. A. Trujillo
4552 M. G. Vigil
4552 H. R. Yoshimura
5500 O. E. Jones
Attn: 5520 T. B. Lane
5521 J. H. Biffle
5522 T. G. Priddy
Attn: R. A. May
5523 R. E. Reuter, Jr.
Attn: D. W. Lobitz
M. J. Sagartz
5800 R. S. Claassen
Attn: 5810 R. G. Kepler
5820 R. E. Whan
5840 N. J. Magnani
5830 M. J. Davis
Attn: 5832 R. W. Rohde
5833 J. L. Jellison
5834 D. M. Mattox
5836 J. L. Ledman
5832 T. J. Lutz (5)
5832 R. J. Salzbrenner
5832 J. W. Munford
5833 G. A. Knorovsky
5835 C. H. Karnes
5835 H. J. Rack (4)
5835 R. E. Blose
5835 J. A. Van Den Avyle
8100 W. J. Spencer
Attn: 8110 J. Barham
8120 W. E. Alzheimer
8150 J. L. Wirth
8160 R. D. Cozine
8310 D. M. Shuster
Attn: 8313 R. W. Mar
8314 L. A. West
8312 W. R. Hoover
Attn: M. W. Mote, Jr.
J. E. Smugeresky
8314 A. J. West
Attn: B. C. Odegard, Jr.
R. E. Stoltz

Unlimited Release
Distribution (continued):

8316 J. C. Swearengen
3141 T. L. Werner (5)
3151 W. L. Garner (3)
For DOE/TIC (Unlimited Release)
4550 TTC Master File
4551 TTC Library (7)
8266 E. A. Aas
DOE/TIC (25)
(R. P. Campbell, 3154-3)

Org.	Bldg.	Name	Rec'd by*	Org.	Bldg.	Name	Rec'd by*

*Recipient must initial on classified documents.